Functional analysis of human adipose tissue-derived mesenchymal stem cells isolated from chronic renal failure patients involved in wound healing

筑　波　大　学

博 士 （医 学） 学 位 論 文

Functional analysis of human adipose tissue-derived mesenchymal stem cells isolated from chronic renal failure patients involved in wound healing

(慢性腎不全患者脂肪組織由来間葉系幹細胞の創傷治癒における機能解析)

２０１７

筑波大学大学院博士課程人間総合科学研究科

VUONG CAT KHANH

Table of contents

Chapter I. General overview

1.1. Background and purposes

Chronic kidney disease, or chronic renal failure (CKD or CRF), with impaired renal function necessitates dialysis or kidney transplantation. Late stages of chronic kidney disease leads to a numerous of complications such as uremia, oxidative stress, anemia, fluid overload which cause a delay in wound healing. Mesenchymal stem cells (MSCs) are considered to be a candidate for wound healing because of the ability to recruit many types of cells. However, it is still unclear whether the CRF-derived MSCs (CRF-AT-MSCs) have the same function in wound healing as healthy donor-derived MSCs (nAT-MSCs). The present study aimed to investigate the effect of uremic toxins, commonly accumulate in CRF patients, to wound healing function of MSCs. Furthermore, I aimed to characterized and analyzed the function of MSCs from adipose tissue of healthy donors and CRF patients in wound healing.

1.2. Material and methods

Firstly, the MSCs isolated from adipose tissues of healthy donors (nAT-MSCs) were analyzed under the treatment of uremic toxins in normoxic and hypoxic conditions. p-cresol, hippuric acid, and indoxyl sulfate were used as the uremic toxins. The expression of reactive oxygen species (ROS) were measured by staining AT-MSCs with 2',7'-dichlorodihydrofluorescein diacetate (H2-DCFDA). The gene and protein levels were performed by quantitative reverse transcription polymerase (qRT-PCR) and Western blot. Then, AT-MSCs from non-diabetic CKD patients stages 3-4 (CKD-AT-MSCs) were characterized by morphology, growth curve, fluorescence-activated cell sorting (FACS) and differentiation assay. Inhibition of ROS was performed by treatment with N-acetyl-L-cysteine (NAC) and inhibition of prolyl-hydroxylase domain protein 2 (PHD-2) was carried out by treatment with IOX2 and small hairpin RNA target PHD-2 (shPHD-2). The flap mouse model was used as in vivo wound healing assays.

1.3. Results

In the present study, I found that uremic toxins induced elevated ROS expression in nAT-MSCs, resulting in the reduced expression of HIF-1α under hypoxic conditions and the impaired wound healing function. Consistent with the uremic-treated AT-MSCs, there was a definite imbalance of redox state and high expression of ROS in CKD-AT-MSCs. Of note, the elevated ROS expression in CKD-AT-MSCs induced prolyl hydroxylase 2 (PHD-2) expression which caused the inhibition of HIF-1α expression. In

addition, a transplantation study clearly revealed that nAT-MSCs promoted the recruitment of inflammatory cells and recovery from ischemia in the mouse flap model, whereas CKD-AT-MSCs had defective functions and the wound healing process was delayed.

1.4. Conclusion

My study provides a tight relationship between the increase of intracellular ROS levels and the impaired activation of HIF-1α and wound healing function of AT-MSCs in both uremic toxin-treated condition or CKD patients. In particular, we show that the expression of prolyl hydroxylase domain 2 (PHD2) is selectively increased in CKD-AT-MSCs and its inhibition successfully restores HIF-1α activation and the wound healing ability in these cells. These results indicate that MSCs from CKD patients need to modify the characteristics before applying for the clinical setting.

1.5. Abbreviations

CRF	chronic renal failure
CKD	chronic kidney disease
GFR	glomerular filtration rate
ESKD	end-stage kidney disease
AT-MSCs	adipose tissue-derived mesenchymal stem cells
nAT-MSCs	AT-MSCs from healthy donors
CRF-AT-MSCs	AT-MSCs from CRF patients
HA	hippuric acid
IS	indoxyl sulfate
NAC	N-acetyl-L-cysteine
IOX2	N-[[1,2-dihydro-4-hydroxy-2-oxo-1-(phenylmethyl)-3 quinolinyl] carbonyl]-glycine
CM-H2DCFDA	2',7'-dichlorodihydrofluorescein diacetate
SDS-PAGE	sodium dodecyl sulfate polyacrylamide gel electrophoresis
PHD-2	prolyl hydroxylase domain protein 1
ROS	reactive oxygen species
HIF-1α	hypoxic inductive factor 1α
SOD1	superoxide dismutase 1
GPX1	glutathione peroxidase 1
VEGF	vascular endothelial growth factor
SDF-1	stromal cell-derived factor 1

Chapter II. Uremic toxins affects the imbalance of redox state and overexpression of prolyl hydroxylase 2 in AT-MSCs involved in wound healing

2.1. Introduction

2.1.1. The accumulation of uremic toxins in chronic kidney disease patients

Kidney plays the vital role in the body to filter the extra water and toxins from the blood by the glomerular filter and balance the body fluids. Chronic kidney disease (CKD) involves the progressive loss of renal function over a period of months or years and results in elevated levels of waste materials, such as urea, creatinine, potassium, in the body, as well as changes in the hormone levels that control blood pressure and the uptake of calcium [1]. The extension of CKD stages leads to the total loss of kidney function and eventually results in mortality [1]. According to the progression of kidney damage, CKD is classified into 5 progressive stages, indicative of organ damage level and reduced glomerular filtration rate (GFR) [1]. In stage 1, when the kidney has normal function but urine findings or structural abnormalities which point to kidney disease are observed, the GFR is still high, over 90 ml/min. The GFR reduces mildly in stage 2, from 60 to 89 ml/min with the mild reduction of kidney function. The kidney function moderately reduced at stage 3, with GFR from 30 to 59 ml/min. Stage 4 is identified when GFR reduces, from 15 to 29 ml/min which is associated with severely reduced kidney function. Stage 5 is considered to be end-stage kidney disease (ESKD), with the GFR less than 15 ml/min and the patients are usually on dialysis [1].

In general, the healthy glomerular filter has the ability to keep the molecules with weights up to 58 kDa [2]. The proteins and small molecules of body waste products were excreted to urine. In renal failure, the glomerular filtration is reduced or the abnormalities in renal metabolism cause the accumulation of a variety compounds which are called uremic toxins [2]. Classically, uremic toxins are divided into three types of molecules [3,4]. The small water-soluble compounds have the molecular weight less than 500 Da and can easily remove by dialysis strategy [3,4]. The protein-bound compounds also have the molecular weight less than 500 Da and have the capacity to bind to proteins which are difficult to remove by dialysis [3,4]. The last group is the middle molecular weight molecules which have the molecular weight more than 500 Da [3,4]. The accumulation of uremic toxins is associated with the progression of CRF and causes the dysfunction of multiple of cell types and organs, thus negatively affects many biological processes [5].

2.1.2. Delay wound healing in CRF patients

Functional renal failure causes the delay of wound healing in CRF patients because of the consequent complications [6-11]. The accumulation of uremic toxins impairs the function of many types of cells contributing to wound healing process [6-8]. Some uremic toxins are known to increase production of the reactive oxygen species level (ROS), a hallmark of uremic syndrome [6-8]. The elevated and sustained ROS causes the sustained pro-inflammatory cytokine secretion, induction of matrix metalloproteases, impairment of dermal fibroblast and keratinocyte function [9,10]. ROS is also known to be involved in the regulation of hypoxic inducible factors which play the central role in wound healing [10]. In ESKD patients who have the severe retention of uremic toxins that leads to uremia, there is the abnormal level of zinc which can promote the wound healing through the auto-debridement and keratinocyte migration [11]. In addition, another complication of CRF such as anemia, which is associated with poor tissue oxygenation, and fluid overloading, which is known as the cause of extensive edema in the lower extremities, are considered as another barrier to wound-healing [11].

Wound healing process consists of four integrated and overlapping phases, hemostasis, inflammation, proliferation and tissue remodeling [12]. Each phase requires the combined activity of growth factors and extracellular matrix proteins, involving with many types of cells such as inflammatory, endothelial, epithelial, and fibroblast cells [12]. These phases of healing can be failed to progress by many factors that cause the impaired healing of wound and ulcers [13]. Most ulcers are associated with ischemia, pressure or metabolic disease as diabetes mellitus, kidney disease [13]. The significant increase number of patients with impaired wound has precipitated the study of the underlying regeneration in wound healing and new therapies for chronic wounds [13].

2.1.3. Stem cell therapy for wound healing delay complication

Up to now, many new therapies for chronic wounds have been being assessed in preclinical and clinical studies [14]. Among them, stem cell therapy is considered as a promising approach for tissue regeneration [15]. However, no stem cell-based therapy has yet gained the approval for the treatment of impaired wound because of many barriers, including the potential risk of immunogenicity and tumorigenicity. The challenge to identify the appropriate stem cell populations for wound therapy

would be necessary to protect and improve the regenerative ability of transplanted stem cells in the wound environments [15,16].

Mesenchymal stem cells (MSCs) are defined as the multipotent progenitor cells that can be expanded *in vitro* and have the potential to differentiate into the mesoderm cell linages [17]. MSCs were first isolated from bone marrow therefore, the bone marrow-derived MSCs (BM-MSCs) have been extensively studied [17]. However, many other sources of MSCs have been reported such as umbilical cord blood, dental pulp, adipose tissues… and it is shown that compared to bone marrow, adipose tissue is an abundant source of MSCs from which the isolation of MSCs is easier, safer and larger amounts of MSCs can be obtained [18,19]. Adipose tissue-derived MSCs (AT-MSCs) are reported to be more genetically and morphologically stable with a lower senescence, higher proliferative capacity and differentiation potential in a long-term culture. In clinical application, AT-MSCs are as effective as BM-MSCs, and in some cases maybe more effective than BM-MSCs [18,19]. The application of MSCs in stem cell therapy has been attracted many studies because of the multipotent to differentiate to a variety of cell linages, the immunomodulatory properties, the safety of usage and lack of ethical issues [20,21].

In wound healing process, MSCs serve a keystone role in recruitment of many other cells in the body to the wound site [22]. MSCs are known to secrete a mixture of growth factors and matrix proteins which are essential for wound healing [23]. Therefore, MSCs are considered to be a promising therapeutic candidate to enhance poor wound healing caused by metabolic disease [22,23].

2.1.4. Effects of uremic toxins and CRF on mesenchymal stem cells characteristics and functions

Transplantation of MSCs into rat models of CRF resulted in the improvement of renal function [24-26] which suggest that MSCs can be helpful for the treatment strategy of kidney failure. However, several reports suggested that uremic toxins, which are commonly retained in CRF cases, cause the damage of stem cells [27,28]. Treatment with uremic toxins at high concentration causes the negative effect on bone marrow-derived MSCs proliferation and paracrine activity in vitro [27]. Indoxyl sulfate, a protein-bound uremic toxin, causes the impairment of proliferation and induces the senescence at high concentration [28]. However, up to now, the effects of uremic toxins on the function of MSCs, especially in wound healing process, have not been well clarified yet.

Klinkhammer et al. reported that transplantation of bone marrow (BM)-derived MSCs prepared from healthy rat can help to accelerate the healing of glomerular lesions whereas those from CKD rat failed to exhibit such activity [29]. Roemeling-van et al. reported that MSCs derived from adipose tissues (AT-MSCs) of human CRF patients showed no differences in differentiation capacity and stability than those from healthy donors, hinting at autologous use of these cells in CRF therapy [30]. However, Yamanaka et al. reported that adipose-derived MSCs from patients with end-stage kidney disease (ESKD), who have suffered long-term uremia, exhibit downregulation of hypoxic response factors and poor angiogenesis activation [31]. Given that availability of AT-MSCs are superior to other stem cell sources, functional evaluation of patient-derived AT-MSCs is important for autologous cell therapy.

2.1.5. Hypoxic condition, a common condition in wound healing

Hypoxic condition, which can cause physiological and pathological responses in cells, plays an important role in many biological processes [32]. Hypoxic condition is one of the micro-environmental conditions in tissue injury and wound healing. The initial tissue injury causes blood vessel damage and leads to acute hypoxia microenvironment at the wound site [32]. Then, the increased oxygen consumption by infiltrated inflammatory and stromal cells decreases the tissue oxygen tension which leads to chronic hypoxia [32]. Wound healing requires the combined activities of a variety of cells within the injured areas, and the adaption to hypoxic microenvironments of these cells, including inflammatory cells, keratinocytes, endothelial cells, and mesenchymal stem cells, is necessary to exert wound healing activities [32].

Hypoxic stimuli result in the stabilization of a master transcription factor, hypoxia-inducible factor-1α (HIF-1), which regulates the expression of a number of genes related to wound healing [33]. Several studies have shown that the hypoxia-induced activation of HIF-1α is attenuated in CRF-derived MSCs, although the underlying molecular mechanisms have not been fully elucidated [31,34].

Traditionally, HIF-1α is known to be regulated by oxygen-dependent hydroxylase enzymes such as prolyl hydroxylase domain proteins (PHDs) [35-37]. PHDs is a subfamily of dioxygenases that uses oxygen and 2-oxoglutarate as co-substrates, and iron and ascorbate as cofactors [36]. There are three main PHD isoforms, PHD1, PHD2, and PHD3 (also termed EGLN2, EGLN2, and EGLN3, respectively) which share the homologous sequence in the C-terminal catalytic domains while the function of N-terminal is not yet identified, and have the specific

expression patterns [36]. PHD2 is expressed in most tissues whereas PHD1 is present mainly in testes, and few in brain, kidney, heart, and liver; PHD3 is mostly expressed in heart [36]. In the presence of oxygen, PHDs hydroxylate HIF-α subunits, then hydroxylated HIF-a are recognized by the von Hoppel-landau (VHL) protein of the E3 ubiquitin ligase complex and degraded by the polyubiquitination-proteasomal system [36,37]. When intracellular oxygen concentration is reduced, non-hydroxylated HIF-α subunits accumulate and heterodimerize with HIF-1β subunit to form the transcription factors in the nucleus and regulates the expression of many target genes which take important roles in wound healing [36,37].

In addition, recently, many pathways have been reported to be involved in the stability of HIF-1α such as PI3K/Akt, MAPK, mTOR, ROS pathways [38-40]. The electron transport chain performs an essential function in the stabilization of HIF-1α, suggesting that ROS are involved in the regulation of HIF-1α [38-40]. However, the role of ROS in the regulation of HIF-1α is controversial: ROS have been reported to stabilize HIF-1α; and high level ROS expression has been shown to lead to the degradation of HIF-1α in the hypoxic conditions [38-40]. Because the accumulation of ROS is a hallmark of CRF, understanding the role of ROS in the regulation of HIF-1α is important for the use of CKD-AT-MSCs in regenerative medicine.

In the present study, I aimed to analyze the the effects of uremic toxin and CKD on the functions of AT-MSCs in wound healing. In particular, with the central role in wound healing process, hypoxic stimuli were considered as the important condition of the AT-MSCs characteristics in this study.

2.2. Materials and methods

2.2.1. The isolation and culture of adipose tissue-derived mesenchymal stem cells (AT-MSCs)

The studies are conducted according to the amended Declaration of Helsinki. All human cell experiments were approved by the ethics committee of the University of Tsukuba. Human adipose tissues were obtained from non-diabetic stage 3-4 CKD patients (n=5, creatinine level=1.71±0.3, GFR=45.5±9.5 ml/min per 1.73m^2, male, age=74 ± 8 years) and healthy donors who have no diabetic and normal renal function (n=5, creatinine level<1, GFR=95.5±5.5 ml/min per 1.73m^2, male, age=75 ± 8 years) from the Department of Cardiovascular Surgery, University of Tsukuba Hospital, Tsukuba, Japan. Mesenchymal stem cells were isolated from adipose tissues according to a previously described method [41].

Briefly, the adipose tissues were cut into small pieces and incubated in phosphate buffer saline (PBS) containing 0.1% collagenase (Invitrogen, CA) in an hour. The digested tissues were then separated by centrifugation and the cell pellets were re-suspended in culture medium, Iscove's Modified Dulbecco Medium (IMDM, Invitrogen), supplemented with 10% heat-inactivated fetal bovine serum (FBS, Invitrogen), 2 mg/ml L-glutamine (Invitrogen), 100 unit/ml penicillin (Invitrogen) and 5 ng/ml bFGF (Peprotech, UK), and cultured at 37^{o}C in a 5% CO_2 atmosphere.

After every 3 days, the current culture medium which contained non-adherent cells was replaced with the fresh medium and the cells were maintained until reaching 80% confluence. Then, the cells were characterized for MSCs properties and passaged for further experimental purposes. The frozen cell stocks were made using Cell Banker solution (ZENOAQ, Japan) and kept in -80^{o}C overnight, then stored in liquid nitrogen for further experiments. The AT-MSCs used in this study were passaged less than 8 total times.

2.2.2. FACS analysis of AT-MSCs

To purify AT-MSCs, CD45+ and CD31+ cells were eliminated from adherent cells in tissue culture dishes by FACS (MoFlo XDP; Beckman Coulter, State), as described previously [41].

The following antibodies were used for the analysis of AT-MSC markers: Fluorescein isothiocyanate (FITC)-labeled anti-HLA-ABC (311404, BioLegend, CA), FITC-labeled anti-CD90 (328107, BioLegend), FITC-labeled anti-CD34 (555821, BD Biosciences, CA), phycoerythrin (PE)-labeled anti-CD13 (301701, BioLegend), PE-labeled antti-CD166 (559263, BD Biosciences), PE-labeled anti-CD105 (323206, BioLegend), PE-labeled anti-CD73 (550257, BD Biosciences), PE-labeled anti-HLA-DR (307606, BioLegend), PE-labeled anti-CD31 (303106, BioLegend), PE-labeled anti-CD14 (301806, BioLegend), and allophycocyanine (APC)-labeled anti-CD45 (555485, BD Biosciences). FITC-labeled anti-IgG1 (555748, BD Biosciences), APC-labeled anti-IgG1 (555751, BD Biosciences), and PE-labeled anti-IgG1 (555749, BD Biosciences) were used as the isotype controls.

2.2.3. The differentiation of AT-MSCs

AT-MSCs are characterized by their adherence, fibroblast-like morphology and their capacity to differentiate into specific cell lineages, including adipocytes, chondrocytes and osteoblasts [41].

For adipogenic differentiation, cells were cultured in culture medium until 80% confluency, then changed into adipogenic differentiation medium containing 0.1×10^{-6}M dexamethasone (Invitrogen), 0.1mM indomethacin (Invitrogen), and 2 µg/ml insulin (Invitrogen). After 20 days, adipocytic differentiation was confirmed by Oil Red O staining (Wako, Japan).

For chondrogenic differentiation, the cells were incubated at 5×10^4 cells/well in culture medium for 1 h to achieve micromass formation then changed to the medium supplemented with 0.1×10^{-6}M dexamethasone (Invitrogen), 0.25mM ascorbic acid (Invitrogen), 40ng/ml proline (Invitrogen), and 10 ng/ml of transforming growth factor β3 (TGFβ3, Invitrogen) for 7 days. Chondrogenic differentiation was confirmed by hematoxylin and eosin staining (Muto Pure Chemicals, Japan) and Toluidine blue staining (Muto Pure Chemicals) and visualized under a microscope (Olympus, Japan).

For osteogenic differentiation, adherent cells were grown in culture medium until 80% confluency, then changed to osteogenic differentiation medium containing 0.1×10^{-6}M dexamethasone (Invitrogen), 0.2mM ascorbic acid (Invitrogen), and 10mM β-glycerophosphate (Invitrogen). After 20 days of culture, calcium deposits were detected by Alizarin Red staining (Wako).

2.2.4. The cell proliferation assay

AT-MSCs were seeded in 35-mm tissue culture dishes (Sumitomo, Japan) at a density of $5x10^4$ cells/dish in culture medium and cultured for 10 days. The cell culture medium was changed after 3 days. The cells were washed with sterile PBS and treated with 0.05% trypsin/EDTA (Invitrogen) at 24-h intervals for 10 days to separate single cells. Dead cells were excluded using trypan-blue staining solution (Invitrogen) and the numbers of live cells in triplicate dishes were counted using a hemocytometer.

2.2.5. Reverse transcription–polymerase chain reaction (RT–PCR) and quantitative real-time polymerase chain reaction (qRT-PCR)

AT-MSCs were maintained under normoxic conditions until reach 80% confluency. Then, the cells were put under hypoxic condition with 1% oxygen; cells under normoxic condition were used as the control. After 6 hours incubation, cells were collected and AT-MSC total RNA was prepared using Sepasol-RNA I Super G (Nacalai, Japan) according to the manufacturer's instructions. One microgram of

total RNA was reverse transcribed to cDNA using a reverse transcriptase (RT)-polymerase chain reaction (PCR) kit (Toyobo, Japan).

The resulting cDNAs were analyzed using a GeneAmp PCR System (Life technologies, CA) with 23–35 cycles of denaturation at 95^{o}C for 5 seconds followed by anneal and extension at 68^{o}C for 30 seconds then a fluorescence read step. The reaction mixtures for the quantitative PCR were prepared using SYBRGreen Realtime PCR mastermix (Toyobo) and analyzed using a GeneAmp 7500Fast Realtime PCR System (Life Technologies). The sequences of primers used for the PCR reactions are listed in Table 1. The experiments were performed in triplicate and data were calculated by the double delta cycle number of threshold ($\Delta\Delta$Ct) method.

2.2.6. Western blotting

After reaching 80% confluency, AT-MSCs were put under hypoxic condition with 1% oxygen, or kept under normoxic condition as the control. After 8-hour incubation, cells were harvested and nuclear protein was extracted according to the manufacturer's protocol (ThermoFisher Scientific, MA). The extracted protein was then mixed with sodium dodecyl sulfate (SDS) loading buffer (Wako) and heated at 95^{o}C for 3 minutes. Equal amounts of protein were separated through SDS–polyacrylamide gels and transferred onto PVDF membranes (EMD Millipore, Germany) for Western blotting.

Then, the membranes were immunoblotted with primary antibodies, including rabbit anti-Hypoxic-inducible factor-1α (HIF-1α) (NB100-105, Novus Biologicals, CO) and rabbit anti-prolyl-hydroxylase domain-2 (PHD-2) (D31E11, Cell Signaling Technology, MA) . Goat anti-Lamin B antibody (sc-6217, Santa Cruz Biotechnology, CA) was used to monitor protein loading and transfer. Horseradish peroxidase (HRP)-conjugated rabbit anti-goat IgG (sc-2768, Santa Cruz Biotechnology), and HRP-conjugated goat anti-rabbit IgG (sc2030, Santa Cruz Biotechnology) were used as secondary antibodies. The signals were detected by incubating the membrane with an enhanced chemiluminescence HRP substrate (EMD Millipore) for 1 minute and visualized using an Image Quant LAS 4000 System (GE Healthcare Life Sciences, UK).

2.2.7. Measurement of the intracellular ROS level

The intracellular ROS level of AT-MSCs was measured by staining the cells with ROS indicated reagent, 2',7'-dichlorodihydrofluorescein diacetate (H2-DCFDA,

Invitrogen), according to the manufacturer's instructions. Briefly, after reaching 80% confluency, the culture medium was remove and the cells were washed with PBS and incubated with PBS containing 10μM DCFDA at 37°C for 30 minutes. The fluorescence signal was observed under the microscope and the fluorescence intensity was analyzed by absorbance at 495 nm and 525 nm wavelengths using a photoemission spectrophotometer (Corona Electric, Japan).

2.2.8. The skin flap mouse model

Male C57BL/6 mice were purchased from Charles River Japan, Inc. (Japan), given food and water *ad libitum* and maintained in a 12-hour- light/dark cycle in the Animal Research Center of the University of Tsukuba. All animal experiments were approved by the Animal Care Committee of the University of Tsukuba.

The skin flap mouse models were performed as described previously [42]. Male 10-week-old C57BL/6 mice were anesthetized and the skin on the dorsal surface was cut into a peninsular-shaped incision (3cm × 2cm) to creat an ischemic gradient by blood flow restriction. The mice were divided into 4 groups: no operation (n=5); sham injection with PBS (n=5); nAT-MSCs injection (n=15); and CKD-AT-MSCs injection (n=15). On the first day after the surgical process, a total of $5x10^5$ cells were intramuscularly injected into four divided sites of the flap skin. Cyclosporin-A (20 mg/kg body weight; Wako) was intraperitoneally injected into the mice every 2 days to induce immunosuppression [38].

The wound healing of the flap tissues was analyzed at 2 time points (3-day and 7-day post-transplantation) based on 2 criteria (the inflammatory effect after 3 days of transplantation and the necrotic area after 7 days of transplantation.) After 3 days, mice were sacrificed, the flap tissues were sectioned and stained with inflammatory cell marker, macrophage marker to analyze the inflammatory activity and the function to recruit macrophages. After 7 days, images of the ischemic flaps were captured and the necrotic areas were analyzed using Image J software (NIH, MD). The flap tissues then were sectioned and stained with endothelial markers.

2.2.9. Histological analysis

The frozen flap tissue sections were mounted, stained with hematoxylin and eosin (Wako) and observed under a microscope (Olympus) for the tissue structure. Immunohistochemical staining was used to analyze the function of AT-MSCs in recruiting the inflammatory cells and the vessel formation at the wound sites. The inflammatory cells recruited in the ischemic area were visualized by staining with

PE-labeled anti-CD45 (30F11, BD BioLegend), and PE-labeled anti-Mac1 (561001, BD BioLegend). The vessel formation was identified by staining with PE-labeled anti-31 (557355, BD BioLegend). The numbers of positive cells were counted in ten fields and the average was calculated.

2.2.10. Establishment of PHD-2 knoCRFown MSCs

OmicsLink shRNA Expression Clone targeted to PHD-2 (GeneCopoeia, USA) were treansfected into HEK293T cells using the Lenti-Pac HIV Expression Packaging Kit (GeneCopoeia) and viral particles were collected then infected to target MSCs and selected with puromycin. The PHD-2 expression was confirmed by qRT-PCR.

2.2.11. Statistical analysis

The data were analyzed by ANOVA analysis. SPSS software (IBM Corp., NY) was used to perform the statistical analyses. P values of <0.05 were considered significant. The data are presented as the mean ± standard deviation (SD).

2.3. Results

2.3.1. A temporary treatment of uremic toxins causes the ROS accumulation and reduced expression of antioxidant-related genes in AT-MSCs

It is reported that uremic toxins such as p-cresol (an end-product of protein metabolism and greatly increased in CRF) increase the expression of intracellular ROS in many types of cells [43,44].

Firstly, to investigate the influence of uremic toxin on the redox state of AT-MSCs, I treated the AT-MSCs from normal renal function donors (nAT-MSCs) with p-cresol and evaluated the intracellular ROS level. I observed the change of AT-MSCs morphology before and after treatment and found that treatment with p-cresol at low concentration (20μM) for short periods (24 hours) had no effect on cell viability and morphology under normoxic and hypoxic conditions (Fig. 1A).

To examine the redox state of AT-MSCs under the effect of uremic toxin, the intracellular ROS levels were examined by using CM-H2DCFDA, a ROS indicator (Fig. 1A). I found that the intracellular ROS level was greatly increased in the presence of p-cresol under both normoxic and hypoxic conditions (2.3-fold increase under normoxic conditions; 3-fold increase under hypoxic conditions, n=3, P<0.05). Furthermore, the intracellular ROS accumulation was also observed in nAT-MSCs treated with other uremic toxins, hippuric acid (HA) and indoxyl sulfate (IS) (Fig 1B).

In order to examine whether the cells were able to reduce ROS levels following 24-hour period of p-cresol treatment, the nAT-MSCs were continued to culture in the absence of p-cresol and passaged for several times. I found that the elevated ROS levels were decreased to baseline after 6 passages of cells (Fig. 1C).

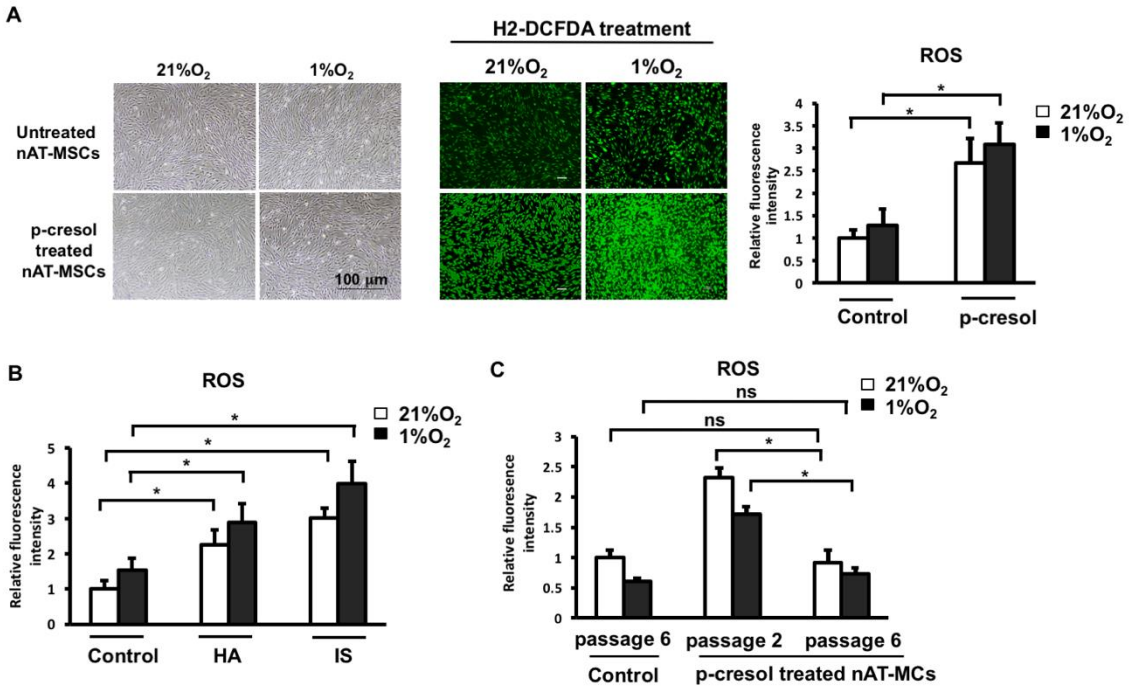

Fig 1. A temporary treatment of uremic toxins causes the reduced ROS accumulation in AT-MSCs. p-cresol, hippuric acid (HA) and indoxyl sulfate (IS) were used as uremic toxins. nAT-MSCs were induced with uremic toxins for 24 hours before analysis. (A) Morphology and ROS level in nAT-MSCs and p-cresol- treated nAT-MSCs. (B) Determination of the influence of HA and IS on ROS level in AT-MSCs. (C) Determination of the reduction of ROS level in nAT-MSCs following p-cresol treatment. The p-cresol-treated nAT-MSCs were continued to culture in the absence of p-cresol and passaged for several times then measured the fluorescence signal of ROS. nAT-MSCs without p-cresol treatment was used as the control. The data represent the mean ± SD. n=3, $^{*}P<0.05$, ns: no significance. The experiments were performed in triplicate. White bar represents the normoxic condition; black bar represents the hypoxic condition.

MSCs are known to constitutively express high levels of antioxidant enzymes, which can regulate the balance of intracellular ROS [46]. Next, I checked the expression of antioxidant enzymes in MSCs under the presence of uremic toxins. As expected, I found that the treatment with p-cresol resulted in a significant reduction of the mRNA expression levels of antioxidant enzyme genes such as SOD1, GPX1 and

catalase in nAT-MSCs under both normoxic and hypoxic conditions (SOD1 expression: 3.4-fold decrease, GPX1: 5.6-fold decrease, catalase: 3.1-fold decrease in the presence of p-cresol under normoxic conditions, n=3, P<0.05) (Fig 2A). Consistent with the decrease of the elevated ROS levels, after nAT-MSCs were continued to culture in the absence of p-cresol and passaged for several times, mRNA levels of antioxidant enzyme genes were restored after 6 passages of cells (Fig 2B).

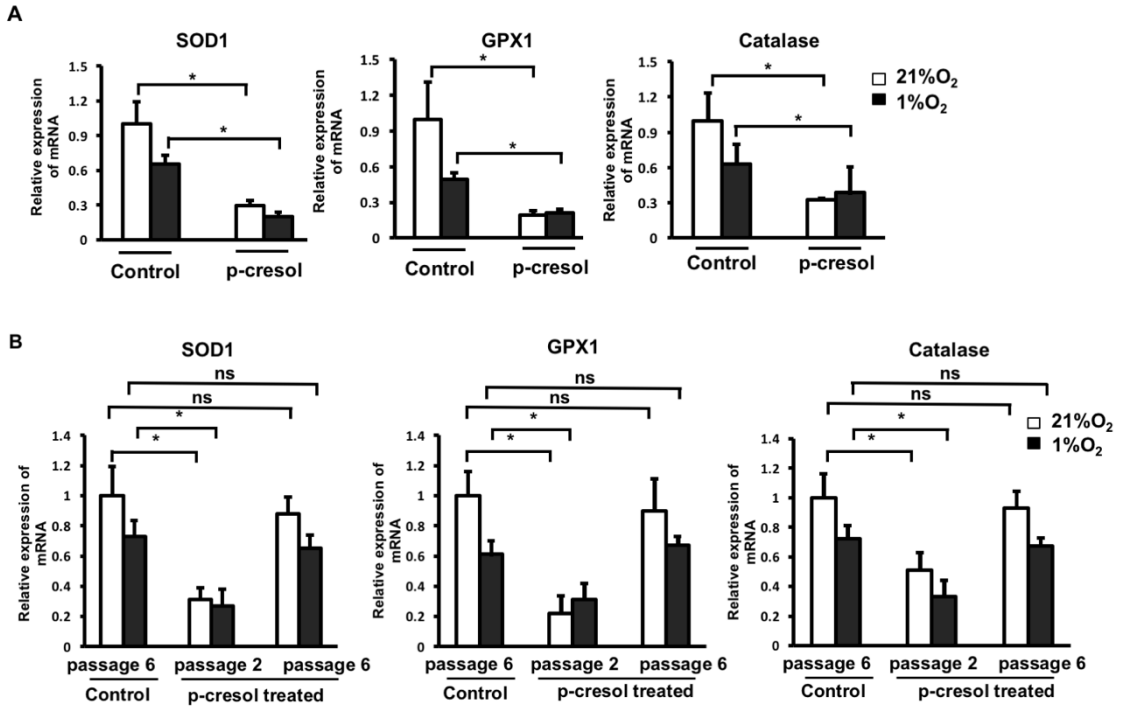

Fig 2. A temporary treatment of uremic toxins causes the expression of antioxidant-related genes. (A) The mRNA expression of antioxidant genes in nAT-MSCs and p-cresol-treated nAT-MSCs. (B) Determination of the recovery of antioxidant enzyme genes expression in nAT-MSCs following p-cresol treatment under normoxic and hypoxic conditions. The p-cresol-treated nAT-MSCs were continued to culture in the absence of p-cresol and passaged for several times then analysed the expression of antioxidant genes. nAT-MSCs without p-cresol treatment was used as the control. The data represent the mean ± SD. n=3, *P<0.05, ns: no significance. The experiments were performed in triplicate. White bar represents the normoxic condition; black bar represents the hypoxic condition.

Collectively, these results indicate that uremic toxins causes the ROS accumulation in nAT-MSCs. The attenuated expression of antioxidant enzyme genes by uremic toxins is the cause of the elevation of ROS in the cells.

2.3.2. A temporary treatment of uremic toxins causes the impaired hypoxic response and loses wound healing activity in AT-MSCs

Hypoxia inducible factor-1α (HIF-1α) is a key transcriptional factor in the response to hypoxic stimuli and regulates the expression of many target genes which play essential roles in the function of MSCs. ROS is known to be involved in the regulation of HIF-1α but the role of ROS in the stability of HIF-1α remains controversial. To investigate whether the induction of intracellular ROS by uremic toxin affects the stability of HIF-1α, I evaluated the mRNA and protein levels of HIF-1α in the uremic toxin-treated nAT-MSCs.

The HIF-1α protein was almost undetectable under normoxic conditions and clearly detected under hypoxic conditions in the untreated nAT-MSCs (Fig. 3A). Remarkably, the HIF-1α protein level was significantly reduced under hypoxic conditions in the uremic toxin-treated cells (Fig. 3A). The HIF-1α mRNA levels were largely unaffected by the p-cresol treatment (Fig. 3A). Consistent with these observations, the mRNA levels of HIF-1α target genes VEGF and SDF-1 were significantly reduced by the p-cresol treatment under hypoxic conditions (VEGF: 3.7-fold decreased expression; SDF-1: 2.3-fold decreased expression, $n=3$, $P<0.05$, Fig. 3B).

My laboratory previously showed that an injection of nAT-MSCs into the injured area facilitates healing process in a mouse skin flap wound model and HIF factors play key roles for the wound healing capability [47,48]. Because both VEGF (which is involved in angiogenesis) and SDF-1 (which is involved in migration) are major factors to promote the wound healing activity, I surmised that the uremic toxin-treated nAT-MSCs may have defective wound healing capability in this model. As expected, the p-cresol treatment almost completely lost the wound-healing effect of nAT-MSCs as revealed by the size of necrotic area on post-transplantation day 7 (uremic toxin-treated nAT-MSCs: 55.08±7.21% vs nAT-MSCs: 28.23±8.05%, $n=3$, $P<0.05$, Fig. 3C). These data indicate that uremic toxins causes the impaired hypoxic response and loses the wound healing activity of nAT-MSCs.

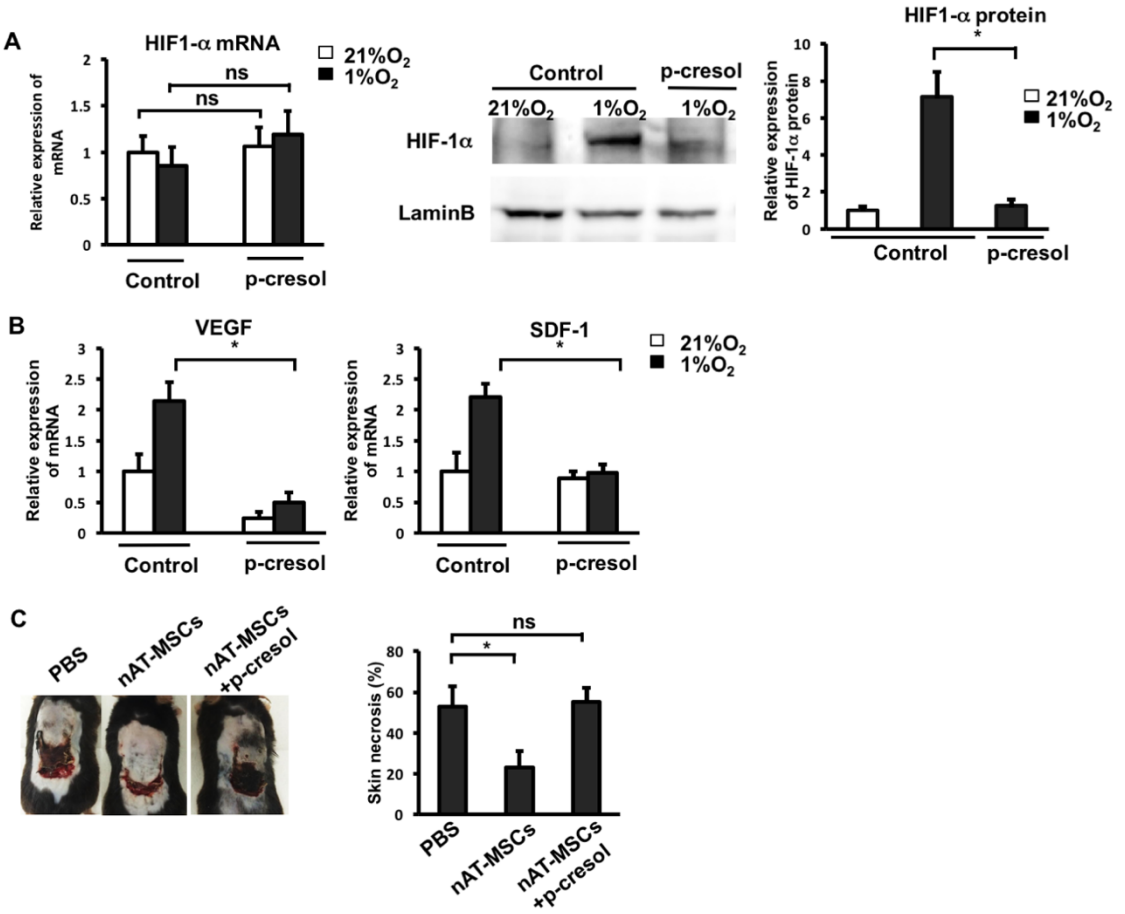

Fig 3. A temporary treatment of uremic toxins causes the impaired hypoxic response and loses wound healing activity in AT-MSCs. (A) The mRNA expression of HIF-1α and HIF-1α protein expression in untreated nAT-MSCs and p-cresol-treated nAT-MSCs. (B) The mRNA expression of VEGF and SDF-1 was determined in untreated nAT-MSCs and p-cresol-treated nAT-MSCs. (C) Necrotic areas of the skin flaps of mice injected with PBS, nAT-MSCs and p-cresol-treated nAT-MSCs on post-transplantation day 7. The data represent the mean ± SD. n=3, *P<0.05, ns: no significance. The experiments were performed in triplicate. White bar represents the normoxic condition; black bar represents the hypoxic condition.

2.3.3. AT-MSCs isolated from the stages 3-4 of CKD patients showed the typical characteristics of mesenchymal stem cells

I next examined AT-MSCs derived from CKD stage 3-4 patients, which supposed to be continuously exposed to uremic toxins in the patient body. Prolonged exposure of uremic toxins often results in the damage of multiple tissues and cell types resulting in secondary organ failure at the terminal stage of CRF. Therefore, to investigate

direct effects of uremic toxins, I have chosen the stage 3-4 of CKD patients as donors of AT-MSCs.

Firstly, I characterized the morphology, proliferation /differentiation abilities, and the expression of MSC cell surface markers of CKD-derived MSCs (CKD-AT-MSCs), comparing with those from non-CKD donors. Both nAT-MSCs and CKD-AT-MSCs had a fibroblast-like morphology, were spindle-shaped, and showed no significant difference in the proliferative ability (Fig. 4A-B). Similar to nAT-MSCs, CKD-ATMSCs expressed the typical markers of MSCs, such as CD13, CD90, CD73, and CD105, and negative with CD31, CD45 markers (Fig. 4C). In addition, CKD-AT-MSCs showed a similar ability to nAT-MSCs to differentiate into osteoblasts, adipocytes and chondrocytes (n=5 in each, P<0.05, Fig. 4D).

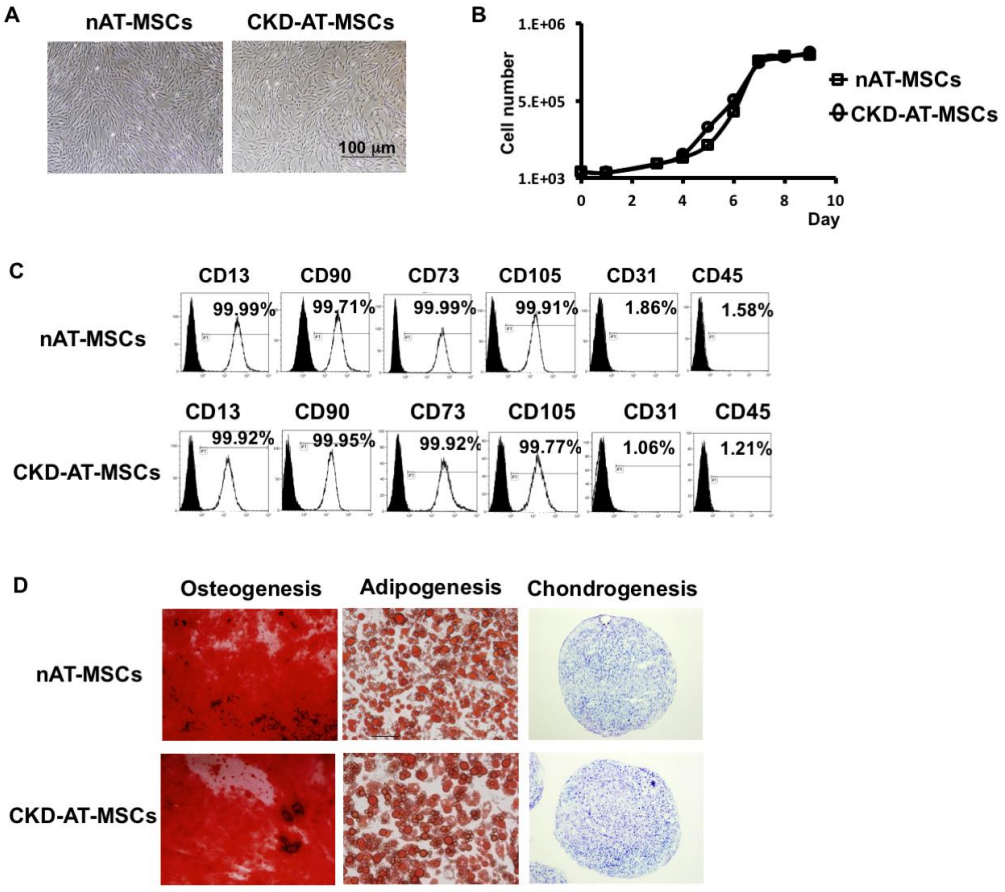

Fig 4. AT-MSCs isolated from CKD patients show the typical characteristics of MSCs. (A) Morphology of AT-MSCs. (B) Growth curve of AT-MSCs. (C) Marker profile of AT-MSCs. (D) Differentiation ability to osteocytes, adipocytes, and chondrocytes of AT-MSCs after 20 days. nAT-MSCs. n=5. The scale bar indicates 100 μm. The experiments were performed in triplicate. Open square represents the nAT-MSCs; open circle represents the CKD-AT-MSCs.

Therefore, I concluded that the AT-MSCs isolated from the CKD patients show the typical MSCs characteristics which have fibroblast-like morphology, expressed typical markers of MSCs, have the ability to proliferate and differentiate to the mesoderm cell lineages, include osteoblasts, adipocytes and chondrocytes.

2.3.4. AT-MSCs isolated from the CKD patients exhibits high levels of intracellular ROS and impaired hypoxic response

To examine that not only treatment under *in vitro* culture, *in vivo* conditions of uremic toxins have the similar influence on AT-MSCs, I then examined whether the intracellular ROS levels were increased in the CKD-derived MSCs as the results I observed in the p-cresol-treated nAT-MSCs.

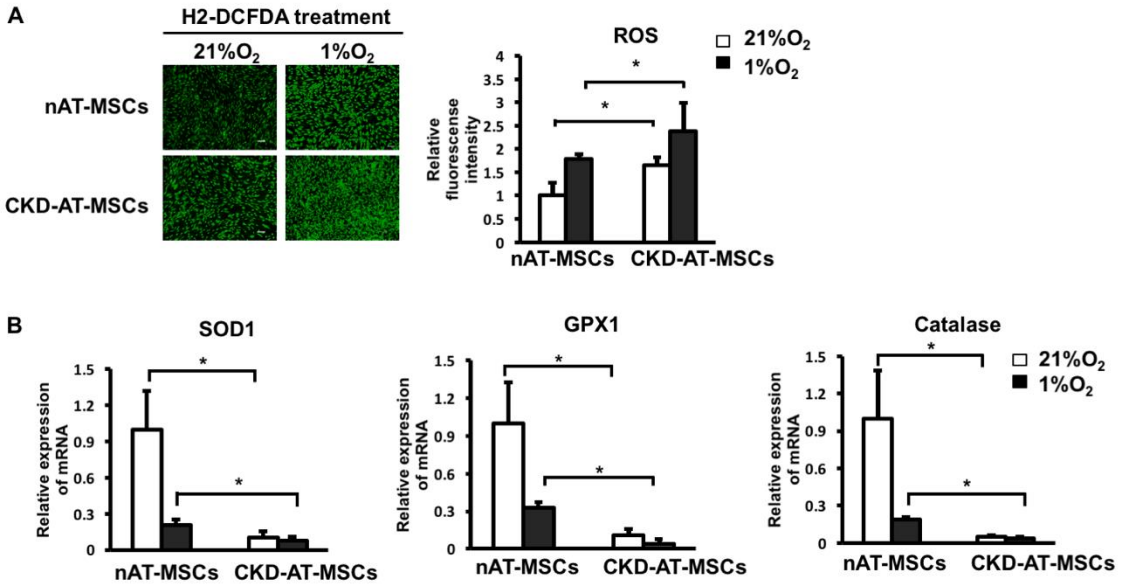

Fig 5. AT-MSCs isolated from CKD patients exhibit high levels of intracellular ROS and impaired antioxidant genes. (A) Determination of intracellular ROS level in AT-MSCs by staining with H2-DCFDA. (B) The mRNA expression of antioxidant genes in AT-MSCs. The data represent the mean ± SD. n=5, *P<0.05, ns: no significance. The scale bar indicates 100 μm. The experiments were performed in triplicate. White bar represents the normoxic condition; black bar represents the hypoxic condition.

I found that even in the absence of the exogenous administration of uremic toxins, the ROS generation in CKD-AT-MSCs was higher than that in nAT-MSCs under both normoxic and hypoxic conditions (2.3-fold higher in normoxic condition and 2.7-fold higher in hypoxic condition, n=4, P<0.05) (Fig. 5A). Moreover, consistent with the case of the p-cresol-treated nAT-MSCs, the mRNA expression levels of

antioxidant enzyme genes (SOD1, GPX1, and catalase) were significantly lower in CKD-AT-MSCs than those in nAT-MSCs (SOD1: 9.72-fold lower; GPX1: 9.23-fold lower; Catalase: 19-fold lower, respectively in AT-MSCs, n=4, P<0.05) (Fig. 5B).

Collectively, these data indicate that the antioxidant ability was severely impaired in CKD-AT-MSCs.

I next examined whether the hypoxic response of HIF-1α protein is altered in the CKD-derived MSCs.

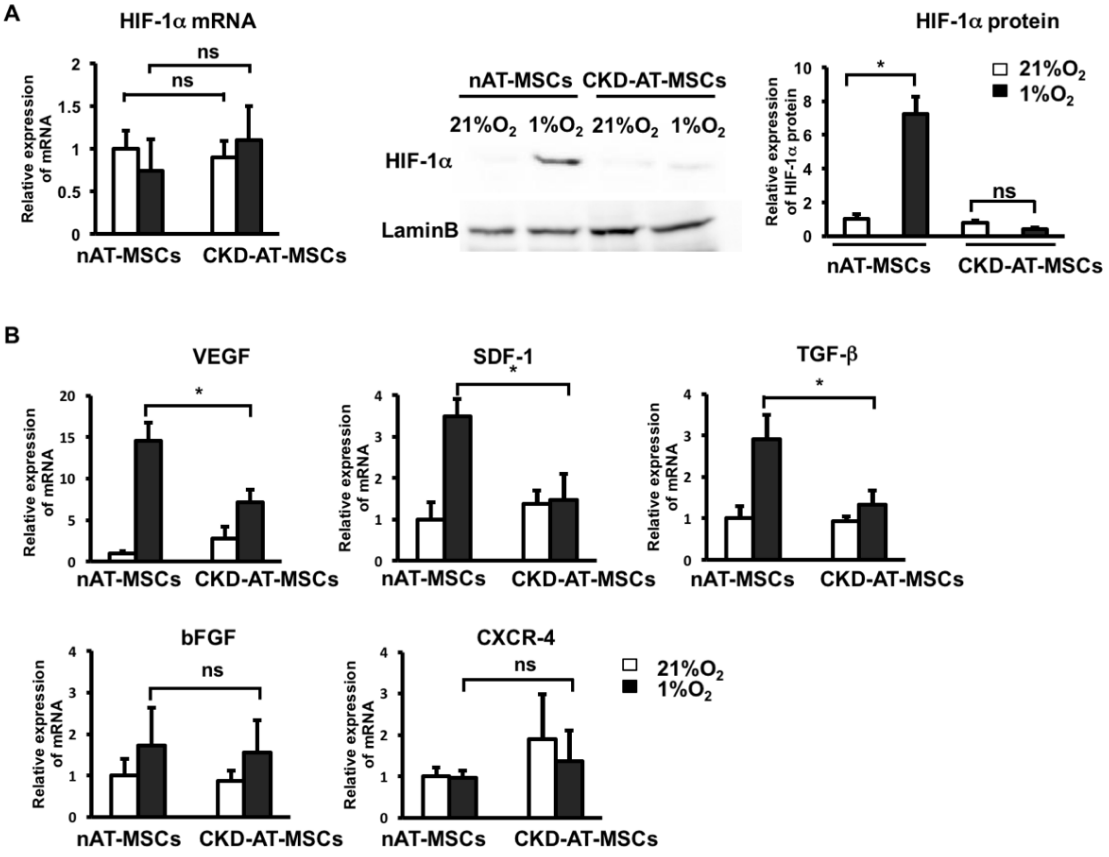

Fig 6. AT-MSCs isolated from the CKD patients have the impaired hypoxic response. (A) The mRNA and protein expression of HIF-1α in AT-MSCs was examined by qRT-PCR and Western blotting, respectively. (B) The mRNA expression of HIF-1α target genes in AT-MSCs. The data represent the mean ± SD. n=5, *P<0.05, ns: no significance. The scale bar indicates 100 μm. The experiments were performed in triplicate. White bar represents the normoxic condition; black bar represents the hypoxic condition.

Similar to the case of the p-cresol-treated nAT-MSCs, the HIF-1α protein level was significantly lower in CKD-AT-MSCs compared to nAT-MSCs under hypoxic conditions, whereas the mRNA expression level was comparable in these cells (Fig.

6A). In association with the reduction of HIF-1α protein, the mRNA levels of VEGF, SDF-1 and TGF-β were significantly reduced under hypoxic conditions (Fig. 6B). By contrast, the moderate increase of bFGF mRNA expression was retained in CKD-AT-MSCs under hypoxic conditions. In addition, the expression of a CXC chemokine receptor CXCR4, another HIF-1α target gene in macrophages, endothelial cells and cancer cells [48], was not increased in nAT-MSCs and CKD-AT-MSCs under hypoxic conditions (Fig. 6B).

2.3.5. CKD-AT-MSCs exhibit impaired wound healing ability

I thought that the reduced expression of HIF-1α target genes might affect the wound healing capacity of CKD-AT-MSCs *in vivo*. To test this possibility, I examined whether an injection of CKD-MSCs into the injured area facilitates healing process as nAT-MSCs did in a mouse skin flap wound model.

Compared to the mice injected with nAT-MSCs, those with CKD-AT-MSCs revealed larger unhealed wound area on post-transplantation day 7 (Fig. 7A). The area of wound site was comparable to the control mice, indicating that CKD-AT-MSCs are incapable of facilitating physiological healing process (the necrotic area: sham control (PBS): 60.02±9.33%, CKD-AT-MSCs: 73.34±7.02% vs nAT-MSCs: 37.52±8.13%, n=3, $P<0.05$).

The histological analysis of wound healing process showed that the numbers of CD45-positive cells and Mac1-positive monocytes/macrophages were significantly increased in the ischemic area of nAT-MSC injected mice on post-transplantation day 3, which indicated that nAT-MSCs possessed a chemoattractive activity that recruited inflammatory cells to the site of tissue damage. In contrast to these observations, lesser numbers of migrated inflammatory cells were observed in CKD-AT-MSC injected mice (CD45-positive cells, CKD-AT-MSCs: 70±14 / field vs nAT-MSCs: 173±19, n=3, $P<0.05$; Mac-1-possitive cells, CKD-AT-MSCs: 66±9 / field vs nAT-MSCs: 158±14, n=3, $P<0.05$, Fig. 7B-C).

On the seventh day of transplantation, the greater number of CD31-positive endothelial cells was appeared in the subcutaneous region of nAT-MSC injected flap compared with that of PBS injected controls. In contrast, when CKD-AT-MSCs were transplanted at the flap site, the number of CD31-positive cells was comparable to the controls (CD31-posstive cells, CKD-AT-MSCs: 438±105 / field vs nAT-MSCs: 1292±291, n=3, $P<0.05$) (Fig. 7C).

Taken together, unlike nAT-MSCs, CKD-AT-MSCs failed to promote the wound healing process throughout the stage in the mouse skin flap wound model.

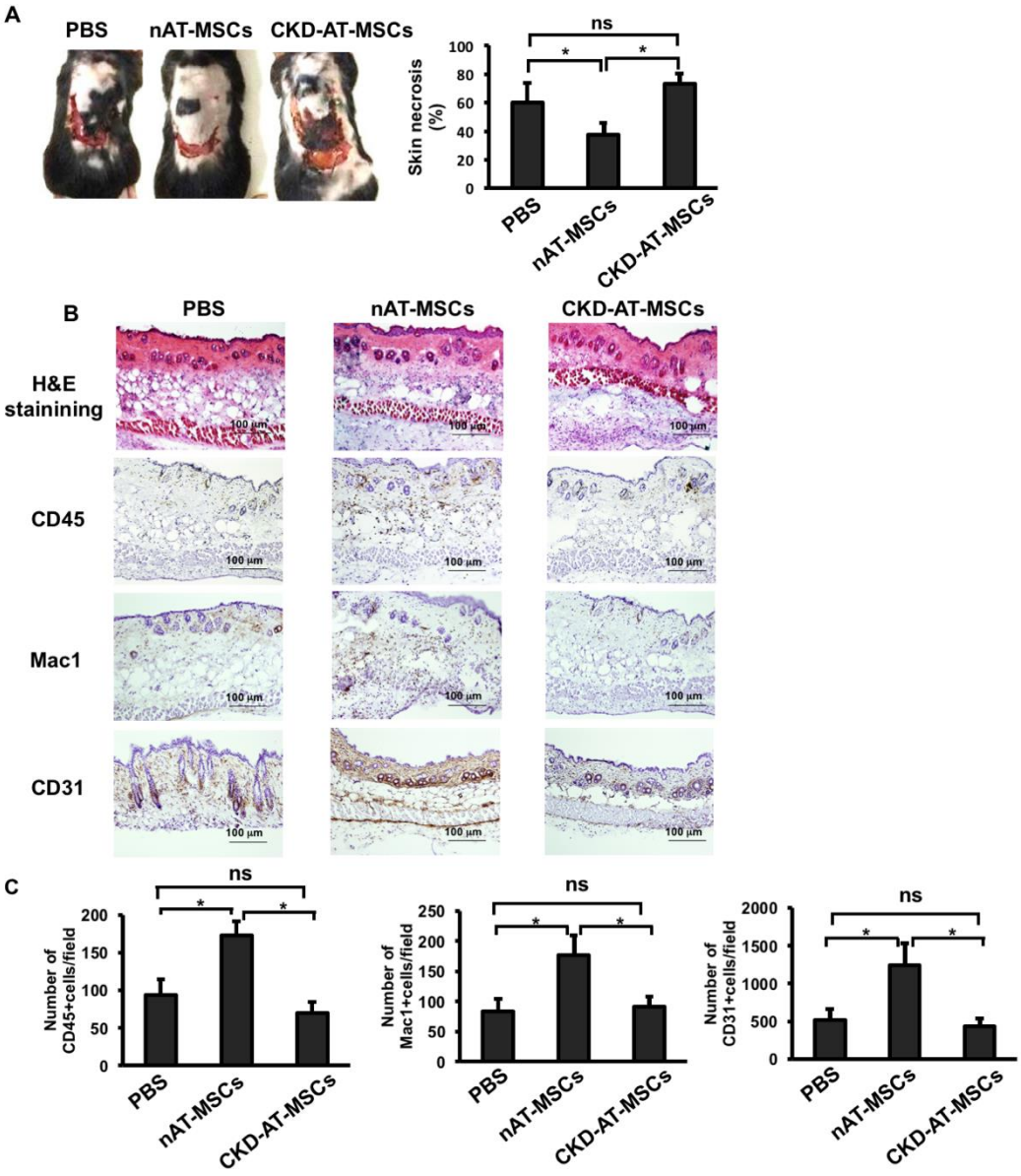

Fig 7. CKD-AT-MSCs exhibit impaired wound healing ability. **(A)** Necrotic areas of skin flaps on post-transplantation day 7. **(B)** The HE staining, PE-labeled anti-CD45, PE-labeled anti-Mac1 on the third day of transplantation and PE-labeled anti-CD31 on the seventh day of transplantation. The data represent the mean ± SD. n=3, *P<0.05, ns: no significance. The experiments were performed in triplicate. The brown dots indicate positive cells.

2.3.6. Treatment of CKD-AT-MSCs with an ROS inhibitor restores the impaired HIF-1α expression under hypoxic conditions

To explore a direct link between the ROS accumulation and the impaired hypoxic response in CKD-AT-MSCs, I next examined whether treatment with an ROS inhibitor (N-acetyl-L-cysteine, NAC) can restore the reduced HIF-1α expression in

CKD-AT-MSCs under hypoxic conditions. CKD-AT-MSCs treated with NAC showed a decrease of intracellular ROS and upregulation of mRNA levels of antioxidant enzymes SOD1, GPX1, and catalase, indicating that the reduced expression of these genes was wholly dependent on ROS (Fig. 8A).

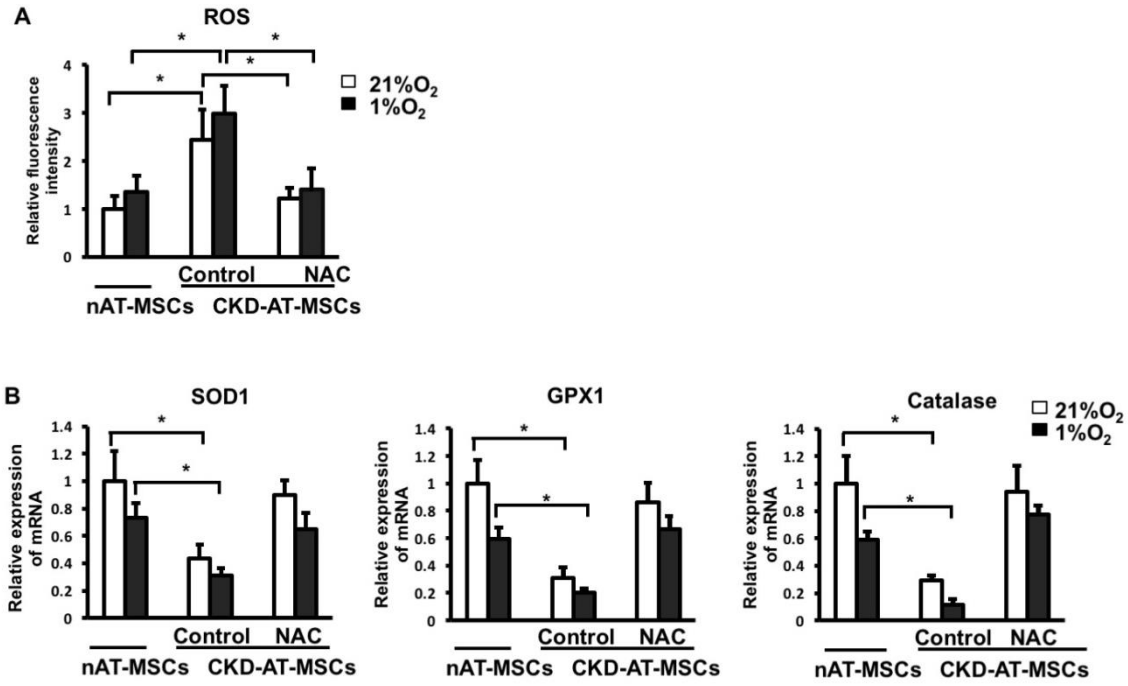

Fig 8. Treatment of CKD-AT-MSCs with an ROS inhibitor restore the oxidative balance. 1M N-acetyl-L-cysteine (NAC) was used as ROS inhibitor. (A) The intracellular ROS level in CKD-AT-MSCs was determined in the absence or presence of a ROS inhibitor under normoxic or hypoxic conditions and compared to nAT-MSCs. (B) The mRNA expression of antioxidant genes in CKD-AT-MSCs was determined in the absence or presence of a ROS inhibitor under normoxic or hypoxic conditions. White bar represents the normoxic condition; black bar represents the hypoxic condition.

Of note, the NAC treatment also restored the hypoxic induction of HIF-1α protein in CKD-AT-MSCs, which was 5.7-fold higher level than that observed in the control cells (n=4, $P<0.05$) (Fig. 9A). Accordingly, the expression of VEGF and SDF-1 was increased in the NAC-treated CKD-AT-MSCs compared to that in the untreated cells under hypoxic conditions (3-fold and 2.5-fold higher, respectively, n=4, $P<0.05$, Fig. 9B). These results strongly indicate that the high level of ROS in CKD-AT-MSCs impairs their wound healing activity by attenuating the hypoxic induction of HIF-1α protein and the expression of hypoxia-inducible genes.

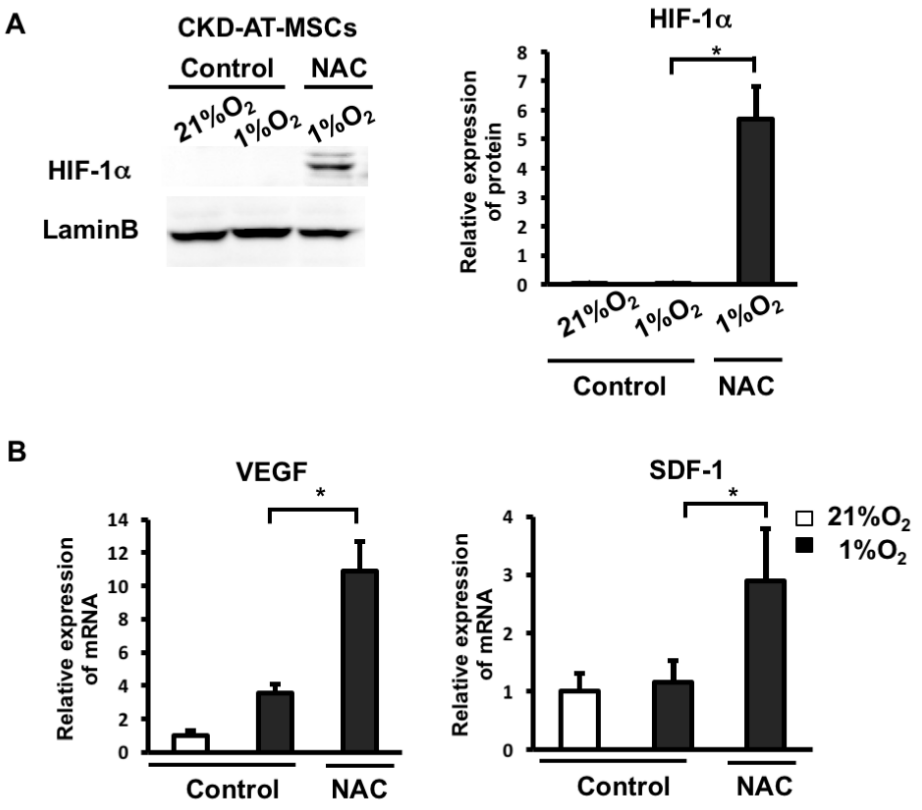

Fig 9. Treatment of CKD-AT-MSCs with an ROS inhibitor restores the hypoxic induction. 1M N-acetyl-L-cysteine (NAC) was used as ROS inhibitor. (A) Western blotting analysis of HIF-1α protein expression in CKD-AT-MSCs. (B) The mRNA expression of VEGF and SDF-1 were determined in CKD-AT-MSCs in the absence or presence of a ROS inhibitor. The data represent the mean ± SD. n=5, *P<0.05. The experiments were performed in triplicate. White bar represents the normoxic condition; black bar represents the hypoxic condition.

2.3.7. Increased expression of prolyl hydrolase domain 2 (PHD-2) is responsible for HIF-1α dysregulation in CKD-AT-MSCs

As shown above, the expression of HIF-1α protein, but not transcript, was decreased both in the p-cresol-treated nAT-MSCs (Fig. 3A) and in CKD-AT-MSCs (Fig. 6A) under hypoxic conditions. To define the molecular basis of these findings, I examined the contribution of the oxygen-responsive prolyl hydroxylases (PHDs) that are known to play key roles in the regulation of HIF-1α protein [50]. PHDs hydroxylate specific proline residues of HIF-1α in the oxygen-dependent degradation (ODD) domain of this protein [50]. This domain is recognized by the von Hippel-Lindau tumor-suppressor protein (VHL), a component of an E3 ubiquitin ligase complex that results

in the rapid proteasomal degradation of HIF-1α [50]. Hypoxia reduces the activity of PHDs, thereby stabilizing HIF-1α protein.

On the basis of these previous findings, I hypothesized that the intracellular accumulation of ROS might keep PHDs in active state, leading to continuous degradation of HIF-1α protein even under hypoxic conditions. To test this possibility, I firstly examined the mRNA levels of PHD genes (PHD1, PHD2 and PHD3) by quantitative RT-PCR. As previously reported [51], the expression of all PHD genes is induced by hypoxia (Fig. 10A). Interestingly, the expression level of PHD-2 was more than doubled in CKD-AT-MSCs compared to that in nAT-MSCs under hypoxic conditions (2.4-fold higher than nAT-MSCs, n=4, P<0.05). On the other hand, those of PHD-1 and PHD-3 were comparable between CKD-AT-MSCs and nAT-MSCs (Fig. 10A). Consistent with the increased mRNA expression, the PHD-2 protein level was increased in CKD-AT-MSCs compared to that in nAT-MSCs under hypoxic conditions (Fig. 10A-B).

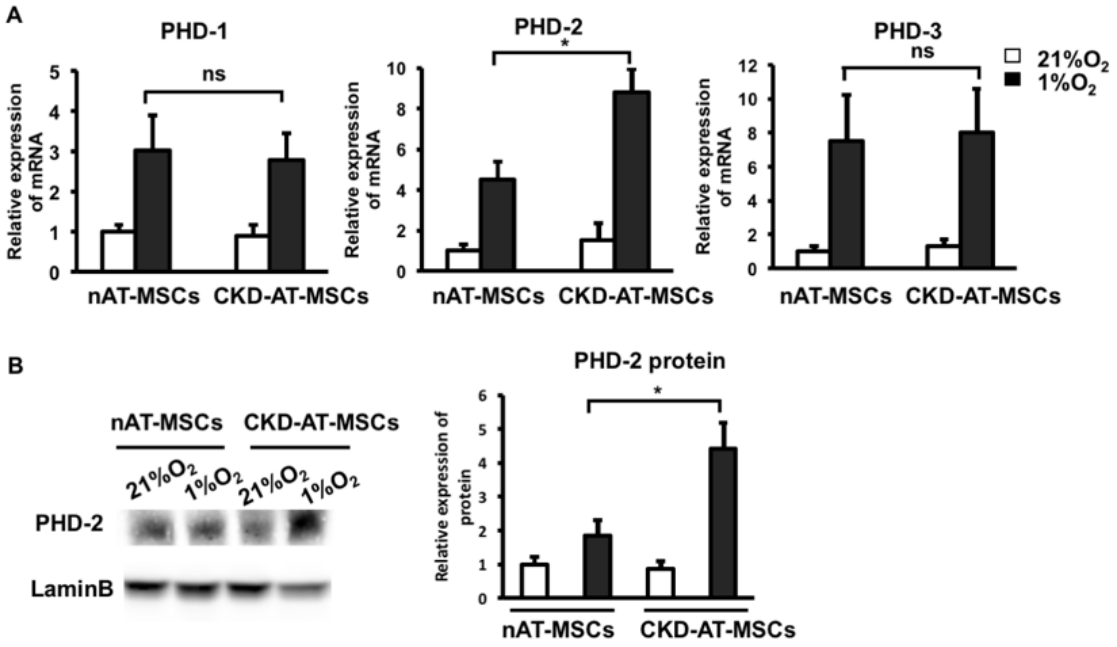

Fig 10. Increased expression of prolyl hydrolase domain 2 (PHD-2) in CKD-AT-MSCs. (A) mRNA expression of PHDs in AT-MSCs. (B) Western blotting of PHD-2 protein expression in AT-MSCs. The data represent the mean ± SD. n=3, *P<0.05, ns: no significance. The experiments were performed in triplicate. White bar represents the normoxic condition; black bar represents the hypoxic condition.

To examine whether the inhibition of PHD-2 is capable of restoring the hypoxia-induced stabilization of HIF-1α protein, CKD-AT-MSCs were pretreated with a PHD-2inhibitor (N-[[1,2-dihydro-4-hydroxy-2-oxo-1-(phenylmethyl)-3-quinolinyl] carbonyl]-glycine, IOX2) and were cultured under hypoxic conditions. As expected, the HIF-1α protein level was higher in the IOX2 treated CKD-AT-MSCs (Fig. 11A). Accordingly, the mRNA levels of VEGF and SDF-1 in CKD-AT-MSCs were significantly higher in these cells (3-fold increase in IOX2-treated CKD-AT-MSCs, n=4, P<0.05, Fig. 11B).

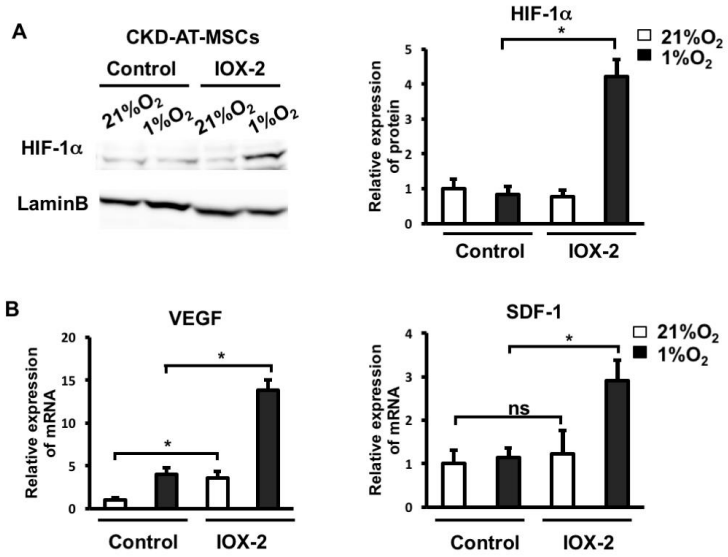

Fig 11. Inhibition of prolyl hydrolase domain 2 (PHD-2) expression restores hypoxic induction in CKD-AT-MSCs. 50 μM IOX2 was used as PHD2 inhibitor. (A) HIF-1α protein expression in CKD-AT-MSCs. (B) The mRNA expression of VEGF and SDF-1 in CKD-AT-MSCs in the absence or presence of PHD-2 inhibitor. The data represent the mean ± SD. n=3, *P<0.05, ns: no significance. The experiments were performed in triplicate. White bar represents the normoxic condition; black bar represents the hypoxic condition.

I further examined whether similar results were observed in CKD-AT-MSCs transduced with small hairprin RNA (shRNA) against PHD-2 gene (KD-PHD-2-CKD-AT-MSCs). The mRNA level of PHD-2 in these cells was reduced to a similar level of that in nAT-MSCs (3.39-fold decrease under normoxic conditions; 2.3-fold decrease under hypoxic conditions, n=3, P<0.05, Fig. 12A). Consistent with the results from IOX2 treated CKD-AT-MSCs, HIF-1α protein was clearly detectable in KD-PHD-2, but not control siRNA transduced CKD-AT-MSCs (Fig. 12B). The mRNA levels of VEGF and SDF-1 in KD-PHD-2-ATMSCs were comparable to those in nAT-MSCs under hypoxic conditions (Fig. 12C). Lastly, I examined whether KD-PHD-2-CKD-AT-MSCs can facilitate wound healing process as nAT-MSCs do in a mouse skin flap

wound model. Indeed, KD-PHD-2-CKD-AT-MSCs showed the recovery of wound healing similar to the control nAT-MSCs (Fig. 12D).

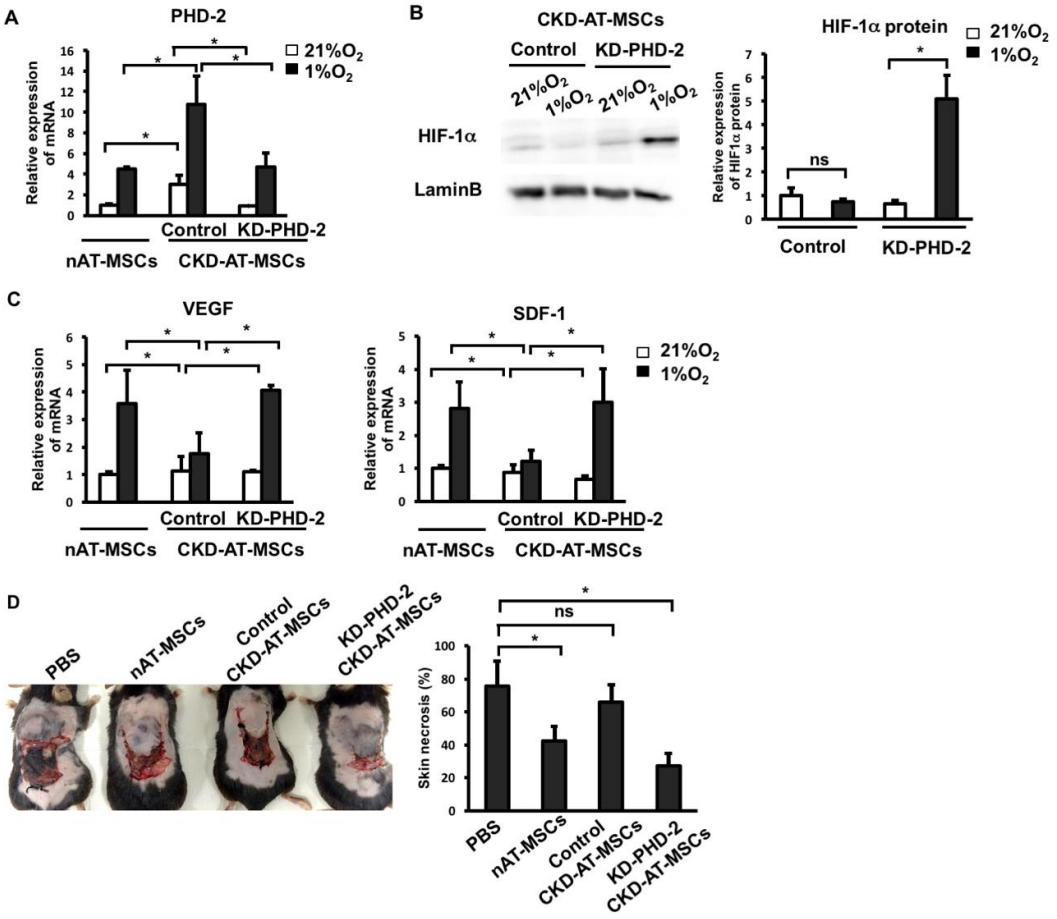

Fig 12. Knockdown of prolyl hydrolase domain 2 (PHD-2) expression restores hypoxic induction and wound healing function of CKD-AT-MSCs. (A) The mRNA expression of PHD-2 in nAT-MSCs, CKD-AT-MSCs (Control) and CKD-AT-MSCs knockdown PHD-2 (KD-PHD-2). (B) HIF-1α protein expression in AT-MSCs. (C) The mRNA expression of VEGF and SDF-1 in AT-MSCs. (D) Necrotic areas of the skin flaps of mice injected with PBS, nAT-MSCs, CKD-AT-MSCs Control and CKD-AT-MSCs KD-PHD-2 on post-transplantation day 7. The data represent the mean ± SD. n=3, *P<0.05, ns: no significance. The experiments were performed in triplicate. White bar represents the normoxic condition; black bar represents the hypoxic condition.

Taken altogether, these data indicate that hypoxic stabilization of HIF-1α protein is impaired in CKD-AT-MSCs accumulating high level of ROS derived from uremic toxins. My data suggest that the impaired hypoxic induction of HIF-1α and functional failure in

wound healing in CKD-AT-MSCs can be restored by inhibition of PHD-2, which is selectively upregulated in these cells.

2.4. Discussion

The present study demonstrated that AT-MSCs isolated from stage 3 and 4 of CKD patients (CKD-AT-MSCs) had an impaired wound healing capacity due to the impaired of antioxidant enzymes and elevated ROS which are involved in the absence of hypoxic induction of HIF-1α protein. The hypoxia responsible genes related to angiogenesis and recruitment of inflammatory cells, such as VEGF and SDF, were downregulated in these cells. Importantly, my data showed that the inability of HIF-1α activation is largely attributed to the increased PHD2 expression in CKD-AT-MSCs under hypoxic conditions. Moreover, correcting the intracellular ROS level restores the hypoxic induction of HIF-1α in these cells, resulting in the recovery of wound healing activity.

2.4.1. Uremic toxins, which accumulated in CRF progression, caused the reversible imbalance of oxidative balance and defective functions of AT-MSCs in wound healing

In CKD patients with progressive impairment of kidney function have the accumulation of uremic toxins [5]. When the uremic toxins amount exceeds in the body, it causes negative impact to organs, tissues, and cells including stem cells. Previous report showed that uremic toxins at high concentration causes the altered paracrine activity of MSCs in vitro, decrease VEGF and TGF-β1 expression which implied the altered function of MSCs [35]. However, the influence of uremic toxins at low concentration on AT-MSCs is not yet identified. In the present study, I clarified whether uremic toxins at low concentration cause any impaired function of AT-MSCs. I focused on the oxidative balance and wound healing functions of AT-MSCs, which are associated with the retention of uremic toxins in CRF. Interestingly, I found that treatment with uremic toxin at low concentration definitely caused the elevated ROS, impaired the hypoxic induction of AT-MSCs and led to the dysfunction of AT-MSCs in wound healing.

To address the underlying mechanism involved in the increased ROS accumulation, I analyzed the antioxidant-related enzymes which maintain the balance of the redox state in the body [52]. Among the antioxidant enzymes controlling the balance of redox state in the cell, superoxide dismutase oxidases (SODs), which catalyze the dismutation of superoxide radicals into either oxygen (O_2) or hydrogen peroxide (H_2O_2), are considered to be one of the most important antioxidant enzymes

[53]. The H_2O_2 is then degraded by other enzymes, such as glutathione peroxidase and catalase [54]. Indeed, I found that uremic toxins impaired the expression of some antioxidant enzymes, including SOD1, GPX1 and catalase, which can explain why the high level of ROS induced the defective wound healing in the AT-MSCs (Fig 1). Importantly, this effect was remained for a short period of time in culture, and was cancelled after prolonged culture.

2.4.2. AT-MSCs derived from stage 3-4 of CKD patients showed the typical characteristics of AT-MSCs, but abnormal ROS expression

Studying the characteristics and functions of AT-MSCs isolated from CRF patients who have the retention of uremic toxins are necessary to apply for clinical therapy, especially auto-transplantation. Up to now, regarding to CRF and MSCs, most of the previous studies used the MSCs isolated from bone marrow or umbilical cord blood which derived from ESKD patients [31, 55]. The accumulation of uremic toxins is a gradual process which begins from the beginning of pathogenesis [5]. Therefore, exacerbations of renal function are associated with the uremic toxins accumulation, with low levels of toxic load and high levels in the end stage [5]. Since I found that even at low concentration uremic toxins caused the defective functions of AT-MSCs, there is a possibility that AT-MSCs derived from the CKD, when the accumulation of uremic toxins is mild and moderate in vivo, also have the similar defect. Therefore, studying the effect of CRF progression on MSCs is required and the data is important for the clinical purpose to apply stem cell therapy to failure progress.

In the present study, I focused on the AT-MSCs isolated from the patients with impaired kidney who are at risk to end stage kidney disease (ESKD). I found that AT-MSCs isolated from CKD patients before ESKD have the typical characteristics of AT-MSCs. Compared to AT-MSCs derived from non-CRF donors, they have the same characteristics in morphology, growth ability, surface marker expression, and differentiation abilities to adipocytes, osteoblasts, and chondrocytes. Interestingly, while cell proliferation, survival and the ability of differentiation were largely unaffected, my data showed that similar to the results of treatment AT-MSCs with uremic toxins in vitro, a significant, but reversible, imbalance of ROS and antioxidant enzymes, including SOD1, GPX1 and catalase, which caused the defective function in wound healing of CRF-AT-MSCs was observed. Although all the samples were derived from cardiovascular disease (CVD) patients who are known to have high level of ROS [56], with the same background of CVD, AT-MSCs from patients with CRF showed

significantly increased expression of ROS compared to non-renal failure cells. This suggested that uremic toxins, a consequent from progressed renal failure, might cause the increase of ROS production in the cells. However, up to now, how uremic toxins regulate the expression of these antioxidant is still unclear. Previously, Bolati et al. showed that indoxyl sulfate, a uremic toxin, downregulates the renal expression of Nrf2 through the activation of NF-κB in the proximal tubular cells and the kidney of a rat model of CRF [58]. NRF-2 is known as a regulator of the expression of direct ROS scavenging enzymes, including SOD1, GPX1 and catalase [59]. Therefore, I hypothesized that Nrf2 might be involved in this pathway; uremic toxins might downregulate the expression of Nrf2, resulting in impaired antioxidant gene expression in CRF-AT-MSCs. Further studies are needed to clarify how uremic toxins effect on the upstream regulators of antioxidant enzymes that lead to the imbalance of redox state in AT-MSCs.

2.4.3. CRF caused the impairment of AT-MSCs function in wound healing from the pre-ESKD by the PHD2/ROS pathway

Recently, Yamanaka *et al.* reported that AT-MSCs from end-stage kidney disease (ESKD) patients who receive long-term dialysis show poor angiogenesis activation [31]. In my study, I found that not only ESKD, which is equivalent with stage 5 of CKD, causes the poor function of AT-MSCs, AT-MSCs isolated from stage 3-4 of CKD showed an impaired wound healing capacity. Consistent with previous report observations in ESKD, I found that HIF-1α and VEGF expression were not upregulated under hypoxic conditions in AT-MSC from CRF. In the case of ESKD patients, the expression of PCAF, a histone acetyltransferase, was significantly downregulated in AT-MSCs [31]. The expression of PCAF is induced by hypoxia in AT-MSCs from healthy controls, but not ESKD patients. Interestingly, I could not find any difference in the expression of PCAF between the CRF-AT-MSCs and nAT-MSCs while both studies showed an impairment of promoting *in vivo* angiogenesis in CRF-AT-MSCs. Furthermore, HIF-1α mRNA levels were comparable between these cells under both normoxic and hypoxic conditions. In addition, inhibition of intracellular ROS level restores the hypoxic induction of HIF-1α and recovered the cells function. Therefore, it is suggested that there is another pathway, related to ROS, which is involved in the impaired function of AT-MSCs from CRF without dialysis.

PHDs are known to act as oxygen sensors whose catalytic activity is oxygen-dependent [59]. My data demonstrated that HIF-1α protein failed to be stabilized even under hypoxic conditions, suggesting that the enzymatic activity of PHDs is persisted,

at least in part, under hypoxic conditions in CRF-AT-MSCs. Therefore, I analyzed the expression of PHDs in CRF-AT-MSCs under hypoxic conditions. Interestingly, I found that only PHD2 expression is specifically increased in CRF-AT-MSCs. Moreover, functional failure of AT-MSCs in wound healing activity was fully restored by inhibiting PHD2 in CRF. Since the impaired activation of HIF-1α is closely associated with an accumulation of intracellular ROS, it is conceivable that ROS is a positive regulator of PHD2. In support of this notion, Hellfritsch *et al*. reported that deletion of mitochondrial thioredoxin reductase (Txnrd2) in mouse embryonic fibroblasts and in tumor cells led to the increased PHD2 protein expression and the absence of hypoxic induction of HIF-1α [60]. In Txnrd2-deficient cells, ROS levels were elevated and PHD2 protein is stabilized via c-Jun NH2-terminal kinase (JNK)-dependent mechanism [60].

Recent studies revealed that the catalytic activity of PHD2 is regulated by a complex mechanism involving redox reductions and energy metabolism [61]. Since intracellular ROS is known to oxidize ferrous iron, which is an essential cofactor for PHD-2 [62], the PHD2 activity of might be persisted with ROS accumulation in cells. Taking in other point of view, the enzyme activity of PHD2 is also known to be dependent on 2-oxoglutarate (2-OG), an intermediate of tricarboxylic acid cycle [62]. Recently, two mitochondrial genes, oxoglutarate dehydrogenase and lipoic acid synthase, were identified as novel HIF-1α regulators [62]. Mutation of these genes results in 2-OG accumulation and L-2-hydroxyglutarate formation, which inhibits the PHD2 activity. The evaluation of oxygen metabolism in the cells with high interacellular ROS level might provide helpful information for understanding the regulation of PHD2 activity.

Another pathway that is considered to regulate PHD-2 expression is the TGFβ1-Smad pathway [63]. TGFβ1 has been shown to induce HIF-1α stabilization through the selective inhibition of PHD-2 expression [63,64]. As shown in Figure 6B, the expression of TGFβ1 was significantly repressed in CRF-AT-MSCs, although the effects of TGFβ1 reduction have not been examined. Although these pathways might explain the increased PHD2 protein level in CRF-AT-MSCs, it remained unsolved that PHD2 mRNA level is also upregulated in CRF-AT-MSCs under hypoxic conditions. Compared to the posttranscriptional regulation, much less is known about the regulation of PHD2 gene transcription. It will be important to address this issue in further studies.

Collectively, these data suggest that mechanisms underlying the impaired hypoxic response in CRF-AT-MSCs might change depending on the pathological stages of CRF.

Chapter III. Conclusion and perspectives

3.1. Conclusions

In the present study, I demonstrated that there is the relation between uremic toxins and oxidative stress in AT-MSCs. Uremic toxins cause the imbalance of intracellular ROS by the declined expression of antioxidant enzymes such as SOD1, GPX1, and catalase. Importantly, the imbalance of ROS induced by uremic toxin causes the impairment of hypoxic induction which causes the lost function of AT-MSCs in wound healing. Graduated accumulation of uremic toxins is a common complication happening preferred of CRF, suggesting that AT-MSCs isolated from CRF patients who have the uremic toxins retention might possess the different characteristics and wound healing functions compared to the normal AT-MSCs.

In addition, I isolated MSCs from CKD patients before dialysis treatment (stage 3-4, CKD-AT-MSCs) to clarify whether under a mild accumulated uremic toxins condition, AT-MSCs were still dramatically impacted. I found that CKD-AT-MSCs show the typical characteristics of mesenchymal stem cells, include morphology, MSCs markers, proliferation and differentiation abilities. Consistent with the results from normal AT-MSCs after treating with uremic toxins, CKD-AT-MSCs showed the imbalance of antioxidant system and high ROS level. Importantly, I found that there is the high expression of PHD2 in CKD-AT-MSCs under hypoxic conditions which cause the lack of HIF-1α protein expression and reduced the expression of HIF-1α target genes related to the angiogenesis and recruitment of inflammatory cells during the wound healing process. The data suggest the negative effect of uremic toxins to the ROS-PHD-2 pathway which related to hypoxic induction and wound healing function in AT-MSCs (Fig. 13).

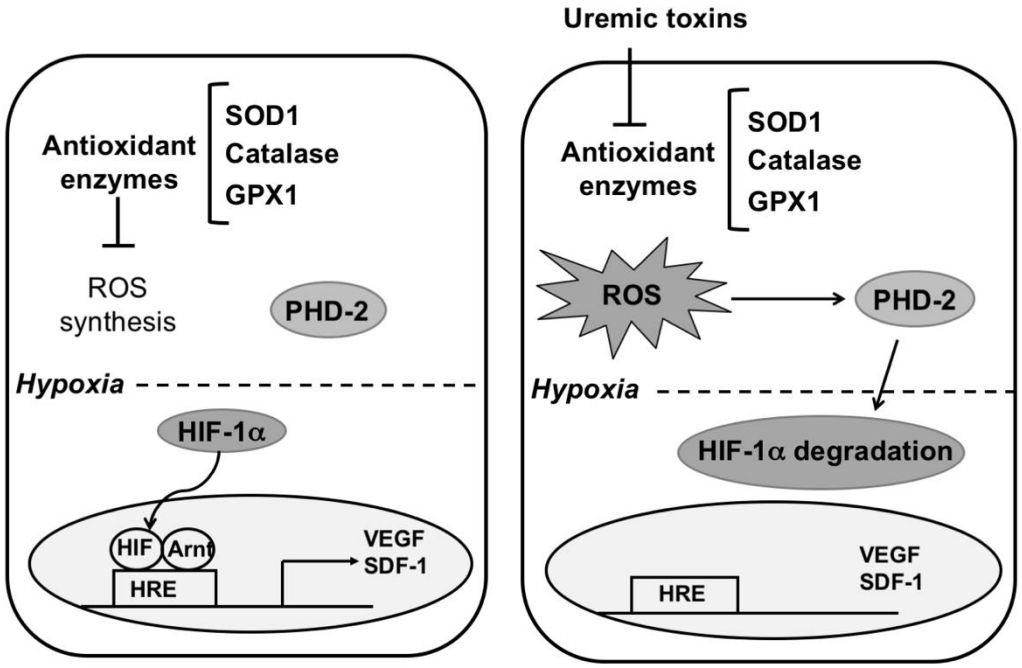

Fig 13. The mechanism underlying the defective function in wound healing of AT-MSCs in CKD patients. In AT-MSCs, there is a balance of the expression of antioxidant enzymes and ROS. Under hypoxic conditions, HIF-1α is stable and induces the expression of target genes involved in wound healing. In contrast, in CKD-AT-MSCs, uremic toxins induced the impairment of antioxidant enzymes, including SOD1, catalase, and GPX1, resulting in a high level of intracellular ROS. ROS can enhance the activity of PHD-2 to hydroxylate HIF-1α and the degradation of HIF-1α occurs even under hypoxic conditions. Consequently, the expression of the target genes involved in wound healing are impaired which results in a loss of wound healing function in CKD-AT-MSCs. HRE: hypoxic response element

3.2. Perspectives

In perspective, my study shows that ROS-PHD-2 pathway may be considered as a therapeutic candidate to modify the function of CKD-AT-MSCs before using in clinical treatment for wound healing delay complication. AT-MSCs isolated from CKD patients had an imbalanced redox state and elevated of PHD-2, and showed the impairment to repair wounds. Pretreatment of CKD-AT-MSCs with IOX2 alone, or in combination with NAC, could be effective to improve their wound healing activity. In addition, my data provide critical information for developing a therapeutic strategy in AT-MSCs-based cell therapy in CKD patients. Special attention should be paid to the pathological stage of CRF, since the wound healing activity of AT-MSCs might be progressively and irreversibly lost at the end stage of CRF.

Tables

Table 1. The background information of patients from whom adipose tissue derived mesenchymal stem cells were isolated

Donner #	Age	Sex	HbA1c	Creatinine (mg/dl)	Stage of CRF
CKD-AT#1	81	M	4.7	1.41	2
CKD-AT#2	77	M	5.5	1.51	2
CKD-AT#3	74	M	5.3	1.64	2
CKD-AT#4	79	M	5.4	2.01	3
CKD-AT#5	66	M	5.7	1.95	3
n-AT#1	68	M	5.8	<1	none
n-AT#2	67	M	4.9	<1	none
n-AT#3	71	M	4.5	<1	none
n-AT#4	82	M	4.6	<1	none
n-AT#5	80	M	5.4	<1	none

Table 2 The primer sets for the quantitative polymerase chain reactions

Function	Gene	Primer	Sequence
Internal control	β-actin	5'-primer 3'-primer	GTGCGTGACATTAAGGAGAAGCTGTGC GTACTTGCGCTCAGGAGGAGCAATGAT
Transcription factor	HIF-1α	5'-primer 3'-primer	GTTTACTAAAGGACAAGTCACC TTCTGTTTGTTGAAGGGAG
	HIF-2α	5'-primer 3'-primer	TGACAGCTGACAAGGAGAAGAA CAGCTCCTCAGGGTGGTAAC
Angiogenic factors, cytokines and chemokines	VEGF	5'-primer 3'-primer	CTACCTCCACCATGCCAAGT GCAGTAGCTGCGCTGATAGA
	SDF-1	5'-primer 3'-primer	TCTGAGAGCTCGCTTGAGTG GTGGATCGCATCTATGCATG
	TGF-β	5'-primer 3'-primer	AGAGCTCCGAGAAGCGGTACCTGAACCC GTTGATGTCCACTTGCAGTGTGTTATCC
	bFGF	5'-primer 3'-primer	AGAGCGACCCTCACATCAAGCTACAAC ATAGCTTTCTGCCCAGGTCCTGTTTTG
	CXCR4	5'-primer 3'-primer	CACTTCAGATAACTACACCG ATCCAGACGCCAACATAGAC

	CXCR7	5'-primer 3'-primer	AAGAAGATGGTACGCCGTGTCGTCTG CTGCTGTGCTTCTCCTGGTCACTGGAC
HIF-1α regulator	PHD-1	5'-primer 3'-primer	GGCGATCCCGCCGCGC CCTGGGTAACACGCC
	PHD2	5'-primer 3'-primer	GCACGACACCGGGAAGTT CCAGCTTCCCGTTACAGT
	PHD-3	5'-primer 3'-primer	ATCGACAGGCTGGTCCTCTA CTTGGCATCCCAATTCTTGT
	p300	5'-primer 3'-primer	GGAAGTGCTGGCAACTTACTG CCATAAGGATTGGGGTTGTTC
	CBP	5'-primer 3'-primer	CTGAGACCCTAACGCAGGTTT GCTGTCCAAATGGACTTGTGT
	PCAF	5'-primer 3'-primer	CTGGAGGCACCATCTCAACGAA ACAGTGAAGACCGAGCGAAGCA
Antioxidant enzymes	SOD1	5'-primer 3'-primer	AATGGACCAGTGAAGGTGTGGGG CACATTGCCCAAGTCTCCAACATGC
	SOD2	5'-primer 3'-primer	ATGTTGAGCCGGGCAGTGTG GTGCAGCTGCATGATCTGCG
	GPX1	5'-primer 3'-primer	CGGCCCAGTCGGTGTATGC CGTGGTGCCTCAGAGGGAC
	Catalase	5'-primer 3'-primer	GAACTGTCCCTACCGTGCTCGA CCAGAATATTGGATGCTGTGCTCCAGG

References

1. Tonelli M, N Wiebe, B Culleton, A House, C Rabbat, M Fok, F McAlister and AX Garg. (2006). Chronic kidney disease and mortality risk: a systematic review. J Am Soc Nephrol 17:2034-47.
2. Huang S-Y, Y-A Chen, S-A Chen, Y-J Chen and Y-K Lin. (2016). Uremic Toxins – Novel Arrhythmogenic Factor in Chronic Kidney Disease – Related Atrial Fibrillation. Acta Cardiologica Sinica 32:259-264.
3. Lisowska-Myjak B. (2014). Uremic Toxins and Their Effects on Multiple Organ Systems. Nephron Clinical Practice 128:303-311.
4. Moradi H, DA Sica and K Kalantar-Zadeh. (2013). Cardiovascular Burden Associated with Uremic Toxins in Patients with Chronic Kidney Disease. American Journal of Nephrology 38:136-148.
5. Ito S and M Yoshida. (2014). Protein-Bound Uremic Toxins: New Culprits of Cardiovascular Events in Chronic Kidney Disease Patients. Toxins 6:665-678.
6. Rutkowski P, EM Slominska, M Szolkiewicz, E Aleksandrowicz, RT Smolenski, W Wolyniec, M Renke, K Wisterowicz, J Swierczynski and B Rutkowski. (2007). Relationship between uremic toxins and oxidative stress in patients with chronic renal failure. Scand J Urol Nephrol 41:243-8.
7. Sung CC, YC Hsu, CC Chen, YF Lin and CC Wu. (2013). Oxidative stress and nucleic acid oxidation in patients with chronic kidney disease. Oxid Med Cell Longev 2013:301982.
8. Oberg BP, E McMenamin, FL Lucas, E McMonagle, J Morrow, TA Ikizler and J Himmelfarb. (2004). Increased prevalence of oxidant stress and inflammation in patients with moderate to severe chronic kidney disease. Kidney Int 65:1009-16.
9. Granata S, A Dalla Gassa, P Tomei, A Lupo and G Zaza. (2015). Mitochondria: a new therapeutic target in chronic kidney disease. Nutrition & Metabolism 12:49.
10. Schafer M and S Werner. (2008). Oxidative stress in normal and impaired wound repair. Pharmacol Res 58.
11. Maroz N and R Simman. (2013). Wound Healing in Patients With Impaired Kidney Function. The Journal of the American College of Clinical Wound Specialists 5:2-7.
12. Broughton G, 2nd, JE Janis and CE Attinger. (2006). Wound healing: an overview. Plast Reconstr Surg 117:1e-S-32e-S.
13. Guo S and LA DiPietro. (2010). Factors Affecting Wound Healing. Journal of Dental Research 89:219-229.

14. Sarabahi S. (2012). Recent advances in topical wound care. Indian Journal of Plastic Surgery : Official Publication of the Association of Plastic Surgeons of India 45:379-387.
15. Duscher D, J Barrera, VW Wong, ZN Maan, AJ Whittam, M Januszyk and GC Gurtner. (2016). Stem Cells in Wound Healing: The Future of Regenerative Medicine? A Mini-Review. Gerontology 62:216-225.
16. Sharma RK and JR John. (2012). Role of stem cells in the management of chronic wounds. Indian Journal of Plastic Surgery : Official Publication of the Association of Plastic Surgeons of India 45:237-243.
17. Nombela-Arrieta C, J Ritz and LE Silberstein. (2011). The elusive nature and function of mesenchymal stem cells. Nature Reviews. Molecular Cell Biology 12:126-131.
18. Bunnell BA, M Flaat, C Gagliardi, B Patel and C Ripoll. (2008). Adipose-derived Stem Cells: Isolation, Expansion and Differentiation. Methods (San Diego, Calif.) 45:115-120.
19. Mahmoudifar N and PM Doran. (2015). Mesenchymal Stem Cells Derived from Human Adipose Tissue. In: *Cartilage Tissue Engineering: Methods and Protocols*. Doran PM ed. Springer New York, New York, NY. pp 53-64.
20. Ullah I, Raghavendra B Subbarao and Gyu J Rho. (2015). Human mesenchymal stem cells - current trends and future prospective. Bioscience Reports 35:e00191.
21. Uccelli A, L Moretta and V Pistoia. (2008). Mesenchymal stem cells in health and disease. Nat Rev Immunol 8:726-736.
22. Maxson S, EA Lopez, D Yoo, A Danilkovitch-Miagkova and MA LeRoux. (2012). Concise Review: Role of Mesenchymal Stem Cells in Wound Repair. Stem Cells Translational Medicine 1:142-149.
23. Hocking AM. (2015). The Role of Chemokines in Mesenchymal Stem Cell Homing to Wounds. Advances in Wound Care 4:623-630.
24. Eirin A and LO Lerman. (2014). Mesenchymal stem cell treatment for chronic renal failure. Stem Cell Research & Therapy 5:83-83.
25. Villanueva S, E Ewertz, F Carrion, A Tapia, C Vergara, C Cespedes, PJ Saez, P Luz, C Irarrazabal, JE Carreno, F Figueroa and CP Vio. (2011). Mesenchymal stem cell injection ameliorates chronic renal failure in a rat model. Clin Sci (Lond) 121:489-99.
26. Villanueva S, JE Carreno, L Salazar, C Vergara, R Strodthoff, F Fajre, C Cespedes, PJ Saez, C Irarrazabal, J Bartolucci, F Figueroa and CP Vio. (2013).

Human mesenchymal stem cells derived from adipose tissue reduce functional and tissue damage in a rat model of chronic renal failure. Clin Sci (Lond) 125:199-210.

27. Idziak M, P Pedzisz, A Burdzinska, K Gala and L Paczek. (2014). Uremic toxins impair human bone marrow-derived mesenchymal stem cells functionality in vitro. Exp Toxicol Pathol 66:187-94.
28. Wang W, X Liu, W Wang, J Li, Y Li, L Li, S Wang, J Zhang, Y Zhang and H Huang. (2016). The Effects of Indoxyl Sulfate on Human Umbilical Cord-Derived Mesenchymal Stem Cells In Vitro. Cellular Physiology and Biochemistry 38:401-414.
29. Klinkhammer BM, R Kramann, M Mallau, A Makowska, CR van Roeyen, S Rong, EB Buecher, P Boor, K Kovacova, S Zok, B Denecke, E Stuettgen, S Otten, J Floege and U Kunter. (2014). Mesenchymal Stem Cells from Rats with Chronic Kidney Disease Exhibit Premature Senescence and Loss of Regenerative Potential. PLoS ONE 9:e92115.
30. Roemeling-van Rhijn M, ME Reinders, A de Klein, H Douben, SS Korevaar, FK Mensah, FJ Dor, IJ JN, MG Betjes, CC Baan, W Weimar and MJ Hoogduijn. (2012). Mesenchymal stem cells derived from adipose tissue are not affected by renal disease. Kidney Int 82:748-58.
31. Yamanaka S, S Yokote, A Yamada, Y Katsuoka, L Izuhara, Y Shimada, N Omura, HJ Okano, T Ohki and T Yokoo. (2014). Adipose tissue-derived mesenchymal stem cells in long-term dialysis patients display downregulation of PCAF expression and poor angiogenesis activation. PLoS One 9:e102311.
32. Ruthenborg RJ, J-J Ban, A Wazir, N Takeda and J-w Kim. (2014). Regulation of Wound Healing and Fibrosis by Hypoxia and Hypoxia-Inducible Factor-1. Molecules and Cells 37:637-643.
33. Hong WX, MS Hu, M Esquivel, GY Liang, RC Rennert, A McArdle, KJ Paik, D Duscher, GC Gurtner, HP Lorenz and MT Longaker. (2014). The Role of Hypoxia-Inducible Factor in Wound Healing. Adv Wound Care (New Rochelle) 3:390-399.
34. Noh H, MR Yu, HJ Kim, JS Jeon, SH Kwon, SY Jin, J Lee, J Jang, JO Park, F Ziyadeh, DC Han and HB Lee. (2012). Uremia induces functional incompetence of bone marrow-derived stromal cells. Nephrol Dial Transplant 27:218-25.
35. Bárdos JI and M Ashcroft. (2005). Negative and positive regulation of HIF-1: A complex network. Biochimica et Biophysica Acta (BBA) - Reviews on Cancer 1755:107-120.

36. Fong GH and K Takeda. (2008). Role and regulation of prolyl hydroxylase domain proteins. Cell Death Differ 15:635-41.
37. Yang M, H Su, T Soga, KR Kranc and PJ Pollard. (2014). Prolyl hydroxylase domain enzymes: important regulators of cancer metabolism. Hypoxia (Auckl) 2:127-142.
38. Movafagh S, S Crook and K Vo. (2015). Regulation of hypoxia-inducible factor-1a by reactive oxygen species: new developments in an old debate. J Cell Biochem 116:696-703.
39. Qutub AA and AS Popel. (2008). Reactive oxygen species regulate hypoxia-inducible factor 1alpha differentially in cancer and ischemia. Mol Cell Biol 28:5106-19.
40. Callapina M, J Zhou, T Schmid, R Kohl and B Brune. (2005). NO restores HIF-1alpha hydroxylation during hypoxia: role of reactive oxygen species. Free Radic Biol Med 39:925-36.
41. Kimura K, M Nagano, G Salazar, T Yamashita, I Tsuboi, H Mishima, S Matsushita, F Sato, K Yamagata and O Ohneda. (2014). The role of CCL5 in the ability of adipose tissue-derived mesenchymal stem cells to support repair of ischemic regions. Stem Cells Dev 23:488-501.
42. Ceradini DJ, AR Kulkarni, MJ Callaghan, OM Tepper, N Bastidas, ME Kleinman, JM Capla, RD Galiano, JP Levine and GC Gurtner. (2004). Progenitor cell trafficking is regulated by hypoxic gradients through HIF-1 induction of SDF-1. Nat Med 10:858-864.
43. Schmidt S, TH Westhoff, P Krauser, W Zidek and M van der Giet. (2008). The uraemic toxin phenylacetic acid increases the formation of reactive oxygen species in vascular smooth muscle cells. Nephrol Dial Transplant 23:65-71.
44. Watanabe H, Y Miyamoto, Y Enoki, Y Ishima, D Kadowaki, S Kotani, M Nakajima, M Tanaka, K Matsushita, Y Mori, T Kakuta, M Fukagawa, M Otagiri and T Maruyama. (2015). p-Cresyl sulfate, a uremic toxin, causes vascular endothelial and smooth muscle cell damages by inducing oxidative stress. Pharmacology Research & Perspectives 3:e00092.
45. Valle-Prieto A and PA Conget. (2010). Human mesenchymal stem cells efficiently manage oxidative stress. Stem Cells Dev 19:1885-93.
46. Lee EY, Y Xia, W Kim, MH Kim, TH Kim and KJ Kim. (2009). Hypoxia-enhanced wound-healing function of adipose-derived stem cells: increase in stem cell proliferation and up-regulation of VEGF and bFGF. Wound Rep Regen 17.

47. Nagano M, T Yamashita, H Hamada, K Ohneda, K Kimura, T Nakagawa, M Shibuya, H Yoshikawa and O Ohneda. (2007). Identification of functional endothelial progenitor cells suitable for the treatment of ischemic tissue using human umbilical cord blood. Blood 110:151-60.
48. Trinh NT, T Yamashita, K Ohneda, K Kimura, GT Salazar, F Sato and O Ohneda. (2016). Increased Expression of EGR-1 in Diabetic Human Adipose Tissue-Derived Mesenchymal Stem Cells Reduces Their Wound Healing Capacity. Stem Cells Dev 25:760-73.
49. Schioppa T, B Uranchimeg, A Saccani, SK Biswas, A Doni, A Rapisarda, S Bernasconi, S Saccani, M Nebuloni, L Vago, A Mantovani, G Melillo and A Sica. (2003). Regulation of the chemokine receptor CXCR4 by hypoxia. J Exp Med 198:1391-402.
50. Schofield CJ and PJ Ratcliffe. (2004). Oxygen sensing by HIF hydroxylases. Nat Rev Mol Cell Biol 5:343-54.
51. Metzen E, U Berchner-Pfannschmidt, P Stengel, JH Marxsen, I Stolze, M Klinger, WQ Huang, C Wotzlaw, T Hellwig-Burgel, W Jelkmann, H Acker and J Fandrey. (2003). Intracellular localisation of human HIF-1 alpha hydroxylases: implications for oxygen sensing. J Cell Sci 116:1319-26.
52. Birben E, UM Sahiner, C Sackesen, S Erzurum and O Kalayci. (2012). Oxidative Stress and Antioxidant Defense. The World Allergy Organization journal 5:9-19.
53. Fukai T and M Ushio-Fukai. (2011). Superoxide Dismutases: Role in Redox Signaling, Vascular Function, and Diseases. Antioxidants & Redox Signaling 15:1583-1606.
54. Mates JM. (2000). Effects of antioxidant enzymes in the molecular control of reactive oxygen species toxicology. Toxicology 153:83-104.
55. Noh H, MR Yu, HJ Kim, EJ Jang, ES Hwang, JS Jeon, SH Kwon and DC Han. (2014). Uremic toxin p-cresol induces Akt-pathway-selective insulin resistance in bone marrow-derived mesenchymal stem cells. Stem Cells 32:2443-53.
56. He F, Zuo L. Redox Roles of Reactive Oxygen Species in Cardiovascular Diseases. Miller FJ, ed. *International Journal of Molecular Sciences* 2015; 16(11):27770-27780.
57. Bolati D, H Shimizu, M Yisireyili, F Nishijima and T Niwa. (2013). Indoxyl sulfate, a uremic toxin, downregulates renal expression of Nrf2 through activation of NF-κB. BMC Nephrology 14:1-9.
58. Jung KA and MK Kwak. (2010). The Nrf2 system as a potential target for the development of indirect antioxidants. Molecules 15:7266-91.

59. Berra E, E Benizri, A Ginouvès, V Volmat, D Roux and J Pouysségur. (2003). HIF prolyl-hydroxylase 2 is the key oxygen sensor setting low steady-state levels of HIF-1α in normoxia. The EMBO Journal 22:4082-4090.
60. Hellfritsch J, J Kirsch, M Schneider, T Fluege, M Wortmann, J Frijhoff, M Dagnell, T Fey, I Esposito, P Kölle, K Pogoda, JPF Angeli, I Ingold, P Kuhlencordt, A Östman, U Pohl, M Conrad and H Beck. (2015). Knockout of Mitochondrial Thioredoxin Reductase Stabilizes Prolyl Hydroxylase 2 and Inhibits Tumor Growth and Tumor-Derived Angiogenesis. Antioxidants & Redox Signaling 22:938-950.
61. Niecknig H, S Tug, BD Reyes, M Kirsch, J Fandrey and U Berchner-Pfannschmidt. (2012). Role of reactive oxygen species in the regulation of HIF-1 by prolyl hydroxylase 2 under mild hypoxia. Free Radic Res 46:705-17.
62. Burr Stephen P, Ana SH Costa, Guinevere L Grice, Richard T Timms, Ian T Lobb, P Freisinger, Roger B Dodd, G Dougan, Paul J Lehner, C Frezza and James A Nathan. Mitochondrial Protein Lipoylation and the 2-Oxoglutarate Dehydrogenase Complex Controls HIF1α Stability in Aerobic Conditions. Cell Metabolism 24:740-752.
63. Han WQ, Q Zhu, J Hu, PL Li, F Zhang and N Li. (2013). Hypoxia-inducible factor prolyl-hydroxylase-2 mediates transforming growth factor beta 1-induced epithelial-mesenchymal transition in renal tubular cells. Biochim Biophys Acta 1833:1454-62.
64. McMahon S, M Charbonneau, S Grandmont, DE Richard and CM Dubois. (2006). Transforming growth factor beta1 induces hypoxia-inducible factor-1 stabilization through selective inhibition of PHD2 expression. J Biol Chem 281:24171-81.

Acknowledgements

I sincerely express my gratitude to my advisor, professor Osamu Ohneda, for the kind support during my Doctoral course in University of Tsukuba. I appreciate the time and patience you gave me. From the beginning time of my study till now, you have been given me much valuable advice and motivation in doing research.

I would like to thank to associate professor of University of Science, Dang Thi Phuong Thao, who always follow and support me kindly since I was an undergraduate student.

To fulfill this dissertation, I would like to thank to the thesis committee members, professor Satoru Takahashi, professor Kunihiro Yamagata, associate professor Naoshi Obara, and associate professor Noriko Uesugi for the kind comments and important advice.

I would like to thank to professor Kinuko Ohneda, assistant professor Toshiharu Yamashita and assistant professor Mami Matsuo-Takahashi for your kind support during my experiments and publication. I would like to thank to Dr. Fujio Sato, Dr. Kana Tachi for the support to collect the adipose tissues and patient information.

I greatly appreciate to all members in Prof. Ohneda's Laboratory for your friendship and kind supports, especially my friend Toshiki Kato.

I would like to appreciate to the Japanese Government for providing me the MEXT Scholarship to support my study and life in Tsukuba.

I would like to thank the members of the International office, Medical department office, and Academic Service Office for the Medical Science Area in University of Tsukuba for the help during my school years. I also would like to thank my Vietnamese and international friends who are besides and encourage me during the time staying here.

Finally, I always appreciate my families who are always beside and loving and supporting me. Thank you, my beloved husband, Yukitaka Shimazu, for all your love, understanding and supporting for my study and work.

University of Tsukuba, February 28th 2017 Vuong Cat Khanh